Original Article

Angiotensin II receptor blockers improve endothelial dysfunction associated with sympathetic hyperactivity in metabolic syndrome

Takuya Kishi[a], Yoshitaka Hirooka[b], Satomi Konno[c], and Kenji Sunagawa[c]

Objectives: Renin–angiotensin system inhibitors are preferred for the treatment of hypertension with metabolic syndrome (MetS). Underlying endothelial dysfunction and sympathetic nervous system (SNS) activation are critically involved in the pathogenesis of hypertension in MetS. We investigated whether treatment with angiotensin II type 1 receptor blockers (ARBs) improves endothelial and autonomic function in patients with MetS.

Methods and results: We conducted a prospective, randomized, open-label, blinded endpoint trial. Sixty patients with MetS were randomized into three treatment groups: telmisartan, candesartan, or diet therapy (control; $n=20$ each), and treated for 6 months. To evaluate the endothelial function of forearm resistance arteries, blood flow and vascular resistance were measured using a strain-gauge plethysmograph during intra-arterial infusion of acetylcholine (ACh) or sodium nitroprusside (SNP). At 6 months, both telmisartan and candesartan comparably decreased blood pressure. Furthermore, ARB treatment ameliorated impaired forearm vasodilation in response to ACh. Telmisartan had a greater effect than candesartan on ACh-induced forearm vasodilation. In contrast, forearm vasodilation in response to SNP was comparable between the telmisartan and candesartan-treated groups. ARB treatment increased high-molecular-weight (HMW) adiponectin levels and baroreflex sensitivity, but telmisartan had a stronger effect than candesartan. In addition, only telmisartan treatment significantly decreased plasma norepinephrine concentrations, blood pressure variability, and heart rate variability based on spectral analysis.

Conclusion: These findings indicate that ARBs improve impaired endothelial and baroreflex function, and increase HMW adiponectin levels in patients with MetS. Telmisartan exhibited more beneficial effects than candesartan, and only telmisartan reduced sympathetic hyperactivity, despite similar depressor effects.

Keywords: angiotensin II, autonomic function, endothelial function, metabolic syndrome

Abbreviations: ACh, acetylcholine; ARBs, angiotensin II receptor blockers; BRS, baroreflex sensitivity; FBG, fasting blood glucose; HDL-C, high-density-lipoprotein cholesterol; HMW, high molecular weight; HOMA-IR, homeostasis Model Assessment of Insulin Resistance; LF/HF-HRV, low-frequency power/high-frequency power in heart rate variability; LF-SBPV, LF power/total power in SBP variability (normalized unit); MetS, metabolic syndrome; SNP, sodium nitroprusside; SNS, sympathetic nervous system; TNF, tumor necrosis factor

INTRODUCTION

Metabolic syndrome (MetS) is characterized by visceral obesity, impaired fasting glucose, dyslipidemia, and hypertension [1,2]. Several studies suggest that endothelial function is impaired in MetS [3–6]. Endothelial dysfunction is a predictable marker of cardiovascular events and can be measured in the forearm resistance vessels [7,8] and brachial artery [9–11]. Endothelial dysfunction has not yet been established in MetS [12]. Endothelial dysfunction in the resistance arteries occurs in the early stages of hypertension, and cannot be detected by measurements of flow-mediated vasodilation (used to determine endothelial function of the conduit artery) [13,14], which may lead to contradictory findings in patients with MetS. A recent study demonstrated that endothelium-dependent vasodilation in resistance arteries, but not in the brachial conduit artery, is inversely associated with a 5-year risk of a composite cardiovascular endpoint [15].

Insulin resistance and the sympathetic nervous system (SNS) have important roles in the pathogenesis of MetS [16–19]. Urinary excretion of catecholamine metabolites becomes elevated and more pronounced as the number of symptoms of MetS increases [20]. Sympathetic neural discharge is markedly potentiated [17], leading to increased insulin levels and elevated blood pressure [19]. Thus, treatments targeting the activation of the SNS are reasonable for patients with MetS, because SNS activation enhances

Journal of Hypertension 2012, 30:1646–1655

[a]Department of Advanced Therapeutics for Cardiovascular Diseases, [b]Department of Advanced Cardiovascular Regulation and Therapeutics and [c]Department of Cardiovascular Medicine, Kyushu University Graduate School of Medical Sciences, Fukuoka, Japan

Correspondence to Yoshitaka Hirooka, MD, PhD, FAHA, Department of Advanced Cardiovascular Regulation and Therapeutics, Kyushu University Graduate School of Medical Sciences, 3–1–1 Maidashi, Higashi-ku, Fukuoka 812–8582, Japan. Tel: +81 92 642 5360; fax: +81 92 642 5374; e-mail: hyoshi@cardiol.med.kyushu-u.ac.jp

Received 15 January 2012 **Revised** 23 March 2012 **Accepted** 4 May 2012

DOI:10.1097/HJH.0b013e328355860e

hypertension, insulin resistance [19], and endothelial dysfunction [21]. Furthermore, SNS activation is important for the occurrence and progression of hypertension leading to hypertensive organ damage in MetS [16]. In addition, patients with MetS present with cardiovascular autonomic imbalance, such as reduced baroreflex sensitivity (BRS) [22].

In hypertensive patients with MetS, renin–angiotensin system inhibitors such as angiotensin-converting enzyme inhibitors or angiotensin II receptor blockers (ARBs) are preferred [23,24]. It has not yet been determined, however, whether ARBs have beneficial effects on endothelial and autonomic dysfunction in patients with MetS. The aims of the present study were to investigate whether ARB treatment improves endothelial and autonomic function in patients with MetS, and if so, whether these effects are class effects of ARBs. We divided the patients with MetS into three treatment groups: telmisartan, candesartan, and diet therapy (as a control). Telmisartan and candesartan are widely used long-acting ARBs that have powerful blood pressure-lowering effects [24]. Therefore, we examined endothelial function based on forearm endothelium-dependent vasodilation in response to acetylcholine (ACh) or sodium nitroprusside (SNP) infusion assessed by venous-occlusion plethysmography [25–27]. We also examined autonomic function by measuring plasma norepinephrine concentrations, spectral analysis of blood pressure and heart rate variability, and BRS in patients with MetS before and after 6 months of treatment.

METHODS

This prospective, randomized, open-label, blinded endpoint trial was conducted at Kyushu University Hospital between the period of April 2007 and March 2009. The trial was conducted in accordance with the Declaration of Helsinki. The study protocol and the sample sizes of the patient groups were reviewed and approved by the Ethics Committee for Human Research at our institute. Written informed consent was obtained from each individual prior to participation in the study.

Patients

Sixty patients with MetS (MetS group; 34 men, 26 women; mean age 54 ± 8 years) and 10 non-MetS individuals (six men, four women; mean age 51 ± 6 years) were enrolled in the study. Individuals were recruited from among patients admitted into the Heart Center of Kyushu University Hospital from April 2007 to March 2009. MetS was diagnosed in accordance with the current Japanese criteria [28]; the presence of visceral obesity, defined as waist circumference at least 85 cm in men and at least 90 cm in women, was an essential component in conjunction with two or more of the following criteria: serum triglycerides at least 150 mg/dl, high-density-lipoprotein cholesterol (HDL-C) less than 40 mg/dl, SBP at least 130/85 mmHg, and fasting blood glucose (FBG) greater than 110 mg/dl. Any patient with clinical signs of acute infection, autoimmune disorder, severe renal (serum creatinine level >2.0 mg/dl) or hepatic disease, or suspected malignancy was excluded from the study. In addition, individuals with a history of cardiovascular disease, including coronary artery disease, clinical heart failure, cardiomyopathy, valvular heart disease, stroke, and arteriosclerosis obliterans, were also excluded from the study. Insulin resistance in the patients was determined based on plasma high-molecular-weight (HMW) adiponectin levels and the Homeostasis Model Assessment of Insulin Resistance {HOMA-IR; score = [immunoreactive insulin (μU/ml) × FBG (mg/dl)]/405}. Patients without low HMW adiponectin (<4.0 μg/ml) and high HOMA-IR (>2.5) were excluded from the MetS group. Left-ventricular ejection fraction was determined using the modified Simpson method or the single-plane area-length method on echocardiograms. Twenty-four (MetS) and four (non-MetS) patients had a history of smoking; however, they had all quit smoking after admission to the hospital.

Patients in the non-MetS group were admitted to our hospital for atypical chest pain, fatigue, or palpitations. Careful examination was performed to rule out coronary artery disease (by coronary angiography) and other organic heart diseases (by echocardiogram) or arrhythmia (by Holter electrocardiogram or electrocardiogram monitoring during hospitalization and/or electrophysiological study). After the enrollment interview, some patients in the non-MetS group transiently received some medications such as angiotensin-converting enzyme inhibitors, ARBs, or β-blockers from general practitioners for mild high blood pressure and/or palpitations. The patients did not take these medications continuously, however, and we confirmed that they were not diagnosed with MetS upon admission.

We excluded patients with MetS who had already taken the angiotensin-converting enzyme inhibitors or ARBs used in the present study. Some patients in the MetS group were given calcium channel blockers or statins. Because it is ethically unacceptable to discontinue these medications for study purposes, the medications were discontinued only on the day of the study and were restarted immediately after the study ended. Finally, 60 MetS and 10 non-MetS patients were included in the study. The MetS patients were randomly assigned to receive telmisartan with diet therapy, candesartan with diet therapy, or diet therapy only (as a control) in a 1 : 1 : 1 ratio. Treatment allocation was computer-generated by the server at Kyushu University and operated by the Kyushu University Randomization Service Office using a dynamic allocation method that balanced the factors of sex, age, SBP, forearm vascular resistance, and plasma norepinephrine concentration. Once the eligibility of the patient was confirmed, the investigator contacted the Kyushu University Randomization Service Office and was notified of the allocated treatment. The investigator then assigned the treatment to the patient. An independent adjudication committee blinded to the treatment allocation assessed all of the potential outcomes. Allocation was concealed from the investigators until they contacted the Kyushu University Randomization Service Office.

General procedures

We measured endothelial function and plasma norepinephrine concentration with the patients in the supine

position and in a postabsorptive state at a room temperature between 25 and 27°C before and 6 months after starting treatment. All medications were with-held only on the day of the study. With the patients under local anesthesia, the left brachial artery was cannulated with a 20-gauge intravascular cannula for drug infusion; the cannula was connected to a pressure transducer to directly measure arterial pressure. The antecubital vein was cannulated, and blood samples were obtained for serum or plasma chemistry measurements.

Measurements of forearm blood flow and vascular resistance

Forearm blood flow was measured with a strain-gauge plethysmograph, using the venous-occlusion technique as described previously [25–27]. Forearm blood flow (ml/min per 100 ml of forearm volume) was calculated from the rate of the increase in forearm volume, whereas venous return from the forearm was prevented by inflation of a cuff on the upper arm. The pressure in the venous-occlusion or congesting cuff was 40 mmHg. Circulation to the hand was arrested by inflating a cuff around the wrist. The mean of four measurements made at 15-s intervals was used for the subsequent analysis. Forearm vascular resistance was calculated by dividing the mean arterial pressure (DBP and one-third of the pulse pressure in mmHg) by forearm blood flow. Forearm vascular resistance is expressed in units. Forearm blood flow, arterial pressure, and heart rate were measured at rest and during the administration of graded doses of ACh (4, 8, or 16 μg/min) or SNP (0.4, 0.8, or 1.6 μg/min). Each dose of ACh or SNP was infused for 5 min, and forearm blood flow was measured after each infusion.

Assessment of autonomic function

As parameters of autonomic function in the present study, we measured plasma norepinephrine concentrations, spectral analysis for SBP and heart rate variability, and BRS. Blood pressure was monitored using the TaskForce Monitor 3040i (CNSystems, Graz, Austria). The cuff was attached to a finger on the left hand that was supported at the heart level. Electrocardiogram electrodes were attached to the chest. After a minimum of 5 min and once the blood pressure and heart rate readings had stabilized, we obtained three consecutive 5-min recordings of blood pressure and electrocardiogram tracing. Noninvasive brachial blood pressure readings were taken with an appropriately sized cuff. We calculated the low frequency (<0.15 Hz) power/high frequency (0.15–0.4 Hz) power in heart rate variability ratio (LF/HF-HRV) as an indicator of sympatho-vagal balance and the low-frequency power/total power in SBP variability ratio (normalized unit; LF-SBPV) as a parameter of SNS activity [29,30]. Sequence analysis detected sequences of three or more beats during which there was either an increase in SBP and pulse interval (up sequence) or a decrease in SBP and pulse interval (down sequence). BRS was estimated as the mean slope of the up-sequences (Up BRS) and down-sequences (Down BRS), and the mean slope of all sequences was determined as BRS (Sequence BRS) [31,32].

Treatments

All patients in the present study received individual nutritional education every month. The education was performed by the same nutritional instructor, and all patients were asked to follow the calorie-controlled Dietary Approaches to Stop Hypertension diet plan, which emphasizes vegetables, fruits, whole grains, lean meats, and low fat dairy food, and foods rich in magnesium, potassium, calcium, and fiber. The patients were asked to record their daily dietary intake, which was checked by the instructor every month. The patients in the telmisartan and candesartan-treated groups were treated for hypertension with telmisartan (20–40 mg) or candesartan (4–8 mg), respectively, once a day, and in all of them hypertension was successfully treated (<130/85 mmHg) [24].

Primary and secondary endpoint

The primary endpoint of the study was a statistically significant decrease in the forearm vascular resistance response to ACh at the maximum dose (16 μg/min). The secondary endpoint was a statistically significant reduction of the plasma norepinephrine concentration. These prespecified endpoints were compared between the telmisartan-treated and candesartan-treated groups. An Independent Endpoint Classification Committee, without knowledge of the treatment assignment, reviewed all potential cases and determined whether the cases should be classified as having achieved the primary or secondary endpoint.

Statistical analysis

All results are expressed as mean [standard error of the mean (SEM)]. Values before or after treatment were compared between groups using unpaired *t*-tests. Differences between values before and after treatment were tested for statistical significance using a paired-sample *t*-test. Forearm blood flow and vascular resistance responses to graded doses of ACh or SNP were examined by a repeated-measures analysis of variance (ANOVA). Two-way ANOVA was used to compare forearm blood flow and vascular resistance before and after treatment in the telmisartan-treated and candesartan-treated groups. *P* values less than 0.05 were considered statistically significant.

RESULTS

Patient metabolic profiles before and after treatment

Before treatment, the MetS group had significantly different metabolic profiles compared to the non-MetS group (Table 1), and there were no significant differences among the telmisartan-treated, candesartan-treated, and control groups. Reduction of body weight, FBG, fasting blood insulin, serum triglycerides, and HOMA-IR were similar among telmisartan-treated, candesartan-treated, and control groups (Table 2). The reductions in SBP and high-sensitivity C-reactive protein levels were significantly greater in both the telmisartan and candesartan-treated groups than in the control group, but did not differ between the telmisartan-treated and candesartan-treated groups (Table 2). A reduction in serum uric acid was obtained only in the

TABLE 1. Baseline characteristics

Characteristic	MetS	Control	P
n	60	10	
Age (years)	47 ± 8	51 ± 6	NS
Male/female	34/26	6/4	NS
BMI (kg/m^2)	25.6 ± 1.8	23.4 ± 1.3	<0.01
Waist (cm)	94 ± 5	82 ± 3	<0.01
SBP (mmHg)	148 ± 13	128 ± 9	<0.05
DBP (mmHg)	92 ± 5	78 ± 6	<0.05
Heart rate (b.p.m.)	72 ± 6	68 ± 8	NS
Fasting BG (mg/dl)	118 ± 15	88 ± 14	<0.01
Fasting BI (μU/ml)	17.8 ± 3.9	10.2 ± 4.2	<0.01
HbA1c (%)	6.2 ± 0.7	5.4 ± 0.5	<0.05
Serum LDL-C (mg/dl)	118 ± 16	109 ± 22	<0.05
Serum HDL-C (mg/dl)	38 ± 4	44 ± 5	<0.05
Serum triglyceride (mg/dl)	208 ± 33	138 ± 42	<0.05
Uric acid (mg/dl)	7.2 ± 0.2	5.6 ± 0.4	<0.01
HOMA index	5.2 ± 0.8	2.2 ± 0.4	<0.01
HMW adiponectin (μg/ml)	2.1 ± 0.4	7.4 ± 1.1	<0.01
Serum NE (pg/dl)	436 ± 35	332 ± 33	<0.01
BRS (ms/mmHg)	12.8 ± 1.2	17.6 ± 1.4	<0.01
FBF (ms/min per 100 ml)	4.6 ± 0.4	5.1 ± 0.5	NS
FVR (U)	24 ± 3	19 ± 3	<0.05

BG, blood glucose; BI, blood insulin; BP, blood pressure; BRS, baroreflex sensitivity; FBF, forearm blood flow; FVR, forearm vascular resistance; HDL-C, high-density-lipoprotein cholesterol; HMW, high molecular weight; LDL-C, low-density-lipoprotein cholesterol; NE, norepinephrine; NS, not significant. Values are means ± SEM when appropriate.

telmisartan-treated group (Table 2). The increase in plasma HMW adiponectin levels was significantly greater in both the telmisartan and candesartan-treated groups than in the control group, and significantly greater in the telmisartan-treated group than in the candesartan-treated group (Table 2).

Forearm vascular responses to acetylcholine and sodium nitroprusside

Basal forearm blood flow did not differ between the MetS and non-MetS groups. Basal forearm vascular resistance was significantly higher in the MetS group than in the non-MetS group (Table 1). ACh and SNP evoked significant increases in forearm blood flow and decreases in forearm vascular resistance in a dose-dependent manner (Fig. 1a and b). SBP and heart rate did not change significantly during intra-arterial infusion of ACh or SNP in either group.

Effects of telmisartan and candesartan on basal forearm blood flow and vascular resistance

Basal forearm blood flow did not differ between pretreatment levels and those at 6 months after treatment in the telmisartan-treated and candesartan-treated groups (Table 3). In both the telmisartan-treated and candesartan-treated groups, however, basal forearm vascular resistance was significantly lower at 6 months after treatment than before the treatment (Table 3).

TABLE 2. Patient metabolic profiles before and after treatment

	TLM (*n* = 20)		CND (*n* = 20)		Diet (*n* = 20)	
	Pre	Post	Pre	Post	Pre	Post
BMI (kg/m^2)	25.8 ± 1.7	24.5 ± 1.5	25.6 ± 1.9	24.8 ± 1.8	25.4 ± 1.6	24.7 ± 1.7
Waist (cm)	95 ± 5	92 ± 3	94 ± 5	91 ± 4	94 ± 5	91 ± 2
SBP (mmHg)	147 ± 13	130 ± 9[a]	149 ± 12	131 ± 6[a]	147 ± 11	142 ± 4
DBP (mmHg)	92 ± 4	83 ± 5[a]	93 ± 5	83 ± 4[a]	92 ± 5	89 ± 3
Heart rate (b.p.m.)	71 ± 6	68 ± 4	72 ± 6	68 ± 3	73 ± 6	71 ± 5
Fasting BG (mg/dl)	119 ± 15	104 ± 7	116 ± 16	103 ± 9	117 ± 14	106 ± 6
Fasting BI (μU/ml)	18.2 ± 4.1	13.4 ± 2.1	17.7 ± 3.8	13.6 ± 2.3	17.8 ± 3.8	14.1 ± 2.1
LDL-C (mg/dl)	116 ± 17	112 ± 16	120 ± 15	114 ± 12	117 ± 18	113 ± 11
HDL-C (md/dl)	38 ± 4	41 ± 3	37 ± 3	40 ± 3	38 ± 3	40 ± 2
Triglyceride (mg/dl)	212 ± 35	162 ± 28	208 ± 31	166 ± 31	206 ± 33	172 ± 28
Uric acid (mg/dl)	7.3 ± 0.3	6.5 ± 0.2[a,b]	7.2 ± 0.2	6.7 ± 0.4	7.2 ± 0.2	6.9 ± 0.3
HOMA index	5.3 ± 0.6	3.4 ± 0.3	5.1 ± 0.8	3.5 ± 0.4	5.1 ± 0.8	3.7 ± 0.4
Adiponectin (μg/ml)	2.0 ± 0.4	5.2 ± 0.4[a,b]	2.1 ± 0.3	4.3 ± 0.5[a]	2.1 ± 0.4	3.8 ± 0.6
hsCRP (mg/l)	2.7 ± 0.5	1.3 ± 0.4[a]	2.8 ± 0.6	1.5 ± 0.6[a]	2.8 ± 0.7	2.1 ± 0.8

BG, blood glucose; BI, blood insulin; BP, blood pressure; CND, candesartan; HDL-C, high-density-lipoprotein cholesterol; HMW, high molecular weight; hsCRP, high-sensitive C-reactive protein; LDL-C, low-density-lipoprotein cholesterol; TLM, telmisartan. Values are means ± SEM.
[a]Indicates the significant difference ($P < 0.05$) of the degree of the changes between pretreatment and posttreatment in TLM group, CND group, or diet group.
[b]Indicates the significant difference ($P < 0.05$) of the degree of the changes between pretreatment and posttreatment in CND group compared with those in TLM group.

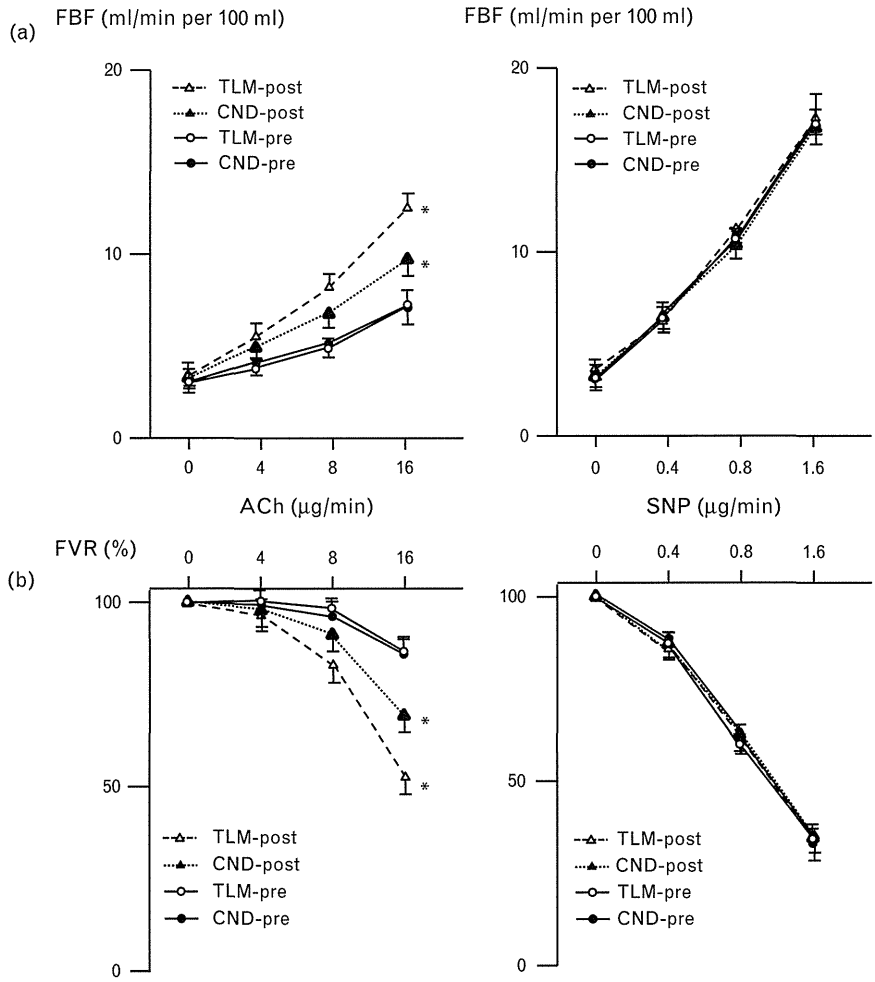

FIGURE 1 (a) Plots showing forearm blood flow (FBF) response to acetylcholine (ACh) or sodium nitroprusside (SNP) in telmisartan (TLM)-treated and candesartan (CND)-treated groups at pre and post-treatment. Results are expressed as mean [standard error of the mean (SEM)]. (b) Plots showing responses of forearm vascular resistance (FVR) to ACh or SNP in TLM-treated and CND-treated groups at pre and post-treatment Results are expressed as mean ± SEM. *$P < 0.05$ between pre and post-treatment in each TLM and CND-treated group.

Primary endpoint

At 6 months after treatment, decreases in the forearm vascular resistance response to ACh at the maximum dose were significantly greater in the telmisartan-treated group than in the candesartan-treated group (Fig. 2). The sample size, 20 patients in each group, is sufficient to detect a difference of 16% in changes in the forearm vascular resistance response to ACh at the maximum dose, with a power of 1-β = 80% and a two-tailed α = 0.05 of 16%.

Secondary endpoint

Plasma norepinephrine concentration was significantly reduced at 6 months after treatment in the telmisartan-treated group, but not in the candesartan-treated group (Fig. 3).

TABLE 3. Parameters of endothelial and sympathetic nervous system activation before and after treatment

	TLM ($n = 20$)		CND ($n = 20$)		Diet ($n = 20$)	
	Pre	Post	Pre	Post	Pre	Post
FBF (ml/min per 100 ml)	4.6 ± 0.4	4.8 ± 0.3	4.5 ± 0.5	4.8 ± 0.2	4.6 ± 0.3	4.7 ± 0.3
Increase in FBF (%)	3 ± 1	10 ± 2[a,b]	3 ± 1	7 ± 1[a]	3 ± 2	4 ± 1
FVR (U)	24 ± 3	21 ± 2[a]	24 ± 2	21 ± 2[a]	24 ± 2	23 ± 3
Decrease in FVR (%)	14 ± 2	50 ± 4[a,b]	13 ± 3	32 ± 3[a]	14 ± 3	16 ± 4
LF/HF-HRV (%)	2.9 ± 0.5	2.2 ± 0.3[a,b]	3.0 ± 0.4	2.7 ± 0.4	3.1 ± 0.5	2.9 ± 0.5
LF-SBPV (%)	58 ± 4	48 ± 4[a,b]	59 ± 5	54 ± 5	58 ± 5	58 ± 6

BRS, baroreflex sensitivity; CND, candesartan; FBF, forearm blood flow; FVR, forearm vascular resistance; LF/HF-HRV, low frequency/high frequency power in heart rate variability; LF-SBPV, low frequency/total power in SBP variability; NE, norepinephrine; TLM, telmisartan. Values are means ± SEM.
[a]Indicates the significant difference ($P < 0.05$) of the degree of the changes between pre and post-treatment in TLM group, CND group, or diet group.
[b]Indicates the significant difference ($P < 0.05$) of the degree of the changes between pre and post-treatment in CND group compared with those in TLM group.

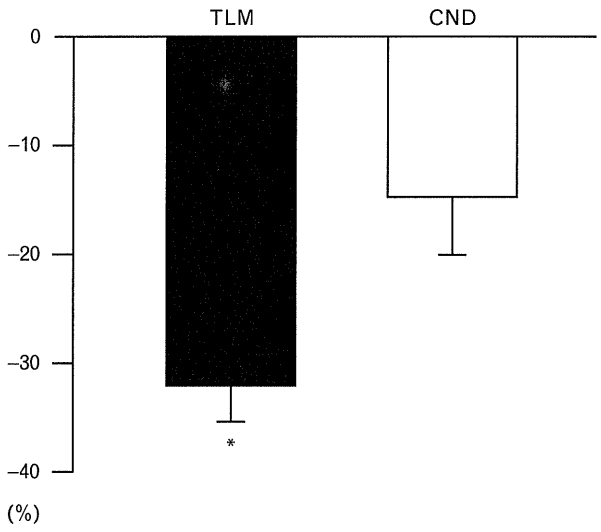

FIGURE 2 Changes in responses of forearm vascular resistance to acetylcholine at 16 μg/min between before and after the treatment in telmisartan-treated (TLM) and candesartan-treated (CND) groups. Results are expressed as mean ± SEM. *$P < 0.05$ in TLM vs. CND.

Effects of telmisartan and candesartan on spectral analysis for SBP and heart rate variability, and baroreflex sensitivity

Low-frequency/high-frequency-HRV and LF-SBPV were significantly reduced at 6 months after treatment only in the telmisartan-treated group (Table 3). BRS was significantly lower in the MetS group than in the non-MetS group before treatment (Table 1). The improvement in BRS at 6 months after treatment was significantly greater in both the telmisartan-treated and candesartan-treated groups than in the control group, and significantly greater in the telmisartan-treated group than in the candesartan-treated group (3.6 ± 1.1 ms/mmHg vs. 1.5 ± 1.0 ms/mmHg vs. 0.7 ± 0.9 ms/mmHg, $n = 20$ for each, $P < 0.05$).

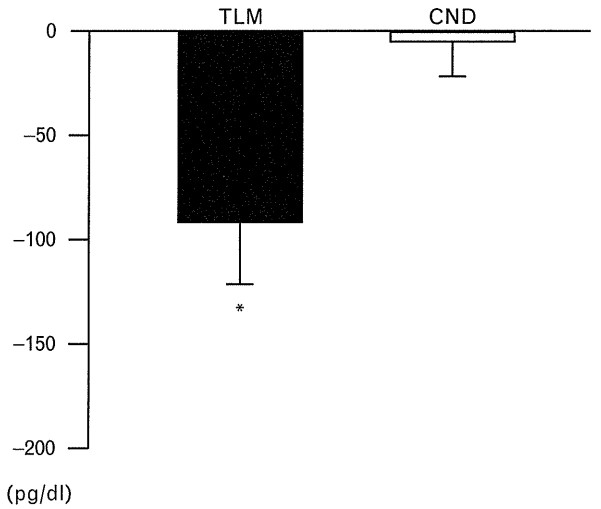

FIGURE 3 Changes in plasma norepinephrine concentration between before and after the treatment in telmisartan-treated (TLM) and candesartan-treated (CND) groups. Results are expressed as mean ± SEM. *$P < 0.05$ in TLM vs. CND.

Relationship between plasma norepinephrine concentrations or baroreflex sensitivity and endothelial function

At the maximum dose of ACh, the decrease in plasma norepinephrine concentrations correlated with the decrease in forearm vascular resistance ($r = 0.72$, $P < 0.002$; Fig. 4a). The increase in BRS was also positively correlated with the decrease in forearm vascular resistance ($r = 0.85$, $P < 0.006$; Fig. 4b).

DISCUSSION

The major findings in the present study are as follows:

1. Treatment with either telmisartan or candesartan ameliorated endothelial dysfunction in patients with MetS. Amelioration of the endothelial dysfunction in the MetS, however, was significantly greater in the telmisartan-treated group than in the candesartan-treated group, despite the similar depressor effects of the two ARBs.
2. Telmisartan, but not candesartan, reduced plasma norepinephrine concentrations, LF/HF-HRV, and LF-SBPV in the patients with MetS.
3. Amelioration of baroreflex dysfunction in patients with MetS was significantly greater in the telmisartan-treated group than in the candesartan-treated group.
4. The increase in HMW-adiponectin in patients with MetS was significantly greater in the telmisartan-treated group than in the candesartan-treated group.

Our findings provide novel insight indicating that ARBs have beneficial effects on endothelial function and baroreflex function in patients with MetS. Moreover, telmisartan inhibited sympathetic hyperactivity in MetS and the sympatho-inhibitory effect might not be a class effect of ARBs.

The findings of the present study demonstrated ARB-induced improvement of endothelial function in forearm resistance arteries, based on the forearm endothelium-dependent vasodilation in response to ACh infusion measured by venous-occlusion plethysmography. Supporting the notion that the endothelial function of resistance arteries is important for cardiovascular outcome, a recent large study of 1016 elderly patients showed reduced forearm endothelium-dependent vasodilation in response to ACh infusion in patients with MetS assessed by venous-occlusion plethysmography [6]. Flow-mediated vasodilation in the brachial artery, however, did not differ between patients with MetS and control individuals [6]. In another recent large study of 1417 men, MetS was not associated with impaired flow-mediated vasodilation [12]. One possible reason for this discrepancy is that endothelial function is impaired earlier in resistance arteries than in conduit arteries, as determined by flow-mediated vasodilation [13,14]. Furthermore, only ACh-induced vasodilation in forearm resistance vessels is a robust predictor of future cardiovascular events during a 5-year follow-up [15]. To predict the future cardiovascular outcome in MetS, we consider that endothelial function of the resistance arteries evaluated by forearm endothelium-dependent vasodilation

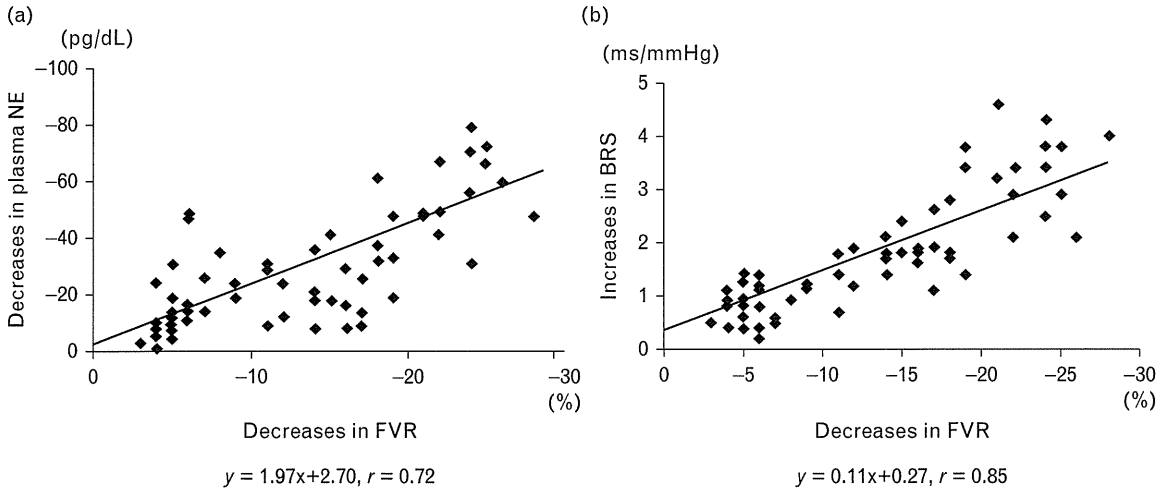

FIGURE 4 Relationship between decreases in plasma norepinephrine (NE) concentrations (a) and the increases in baroreflex sensitivity (BRS) (b) with decreases in forearm vascular resistance (FVR).

in response to ACh would be important in patients with MetS. We previously evaluated forearm vasodilation evoked by ACh using venous-occlusion plethysmography to measure the endothelial function in resistance arteries [25–27]. The present study clearly demonstrates that ARBs improve the endothelial dysfunction based on the response to ACh infusion in patients with MetS, and that the improvement of the endothelial dysfunction was significantly greater in the telmisartan-treated group than in the candesartan-treated group, despite the similar depressor effects of the drugs. These results suggest that ARBs have beneficial effects on endothelial dysfunction in patients with MetS, which might contribute to improve the cardiovascular endpoint in MetS.

The difference between the ARBs in their beneficial effects on endothelial function in patients with MetS is an interesting topic. ARBs are considered to improve endothelial dysfunction via blockade of the angiotensin II pathway; tumor necrosis factor (TNF)-alpha-induced generation of reactive oxygen species, which are inflammation-associated factors; and by decreasing endothelial nitric oxide synthase [33,34]. A previous study demonstrated that vascular endothelial dysfunction is improved by telmisartan to a greater extent than losartan via normalization of the endothelial nitric oxide synthase pathway, nuclear factor-kappa B activation, and TNF-alpha activation [35]. Another study also found that telmisartan, not candesartan, inhibits reactive oxygen species production in a human hepatoma cell line [36]. These results suggest that the beneficial effects on the reduction of oxidative stress and the inflammation-associated factors may differ among ARBs. Although the effects on high-sensitivity C-reactive protein did not differ between telmisartan and candesartan, and oxidative stress was not measured in the present study, the differences between telmisartan and candesartan on the amelioration of endothelial dysfunction in patients with MetS might be related to differences in the antioxidant effects between the two ARBs. Furthermore, in the present study, the effects of telmisartan and candesartan on adiponectin levels were different. Adiponectin levels are independently correlated with endothelium-dependent vasodilation in hypertensive patients [37], as well as in healthy individuals or patients with impaired glucose tolerance [38]. Experimentally, adiponectin inhibits cytokine-induced expression of endothelial adhesion molecules in endothelial cells and reduces atherogenic transformation of macrophages to foam cells by suppressing scavenger receptor expression [37]. We speculate that the difference in the improvement of endothelial dysfunction between the telmisartan and candesartan-treated groups was, at least in part, due to the difference in the improvement of adiponectin levels. The differences in the responses to telmisartan and candesartan were compared using only one dose of each drug and at the trough response of that dose. Although we considered that the similar depressor effects of telmisartan and candesartan after treatment indicated that the appropriate doses of telmisartan and candesartan were used with equal effects, we cannot exclude the possibility that the quantitatively different responses to the ARBs were related to differences in their pharmacokinetic profiles. Moreover, remodeling of resistance arteries is the earliest subclinical alteration that occurs in the vasculature of hypertensive patients and may actually precede endothelial dysfunction. Therefore, further clinical trials are necessary to address these questions.

Another important aspect of MetS is SNS activation. Telmisartan inhibits SNS activation. In the present study, telmisartan, but not candesartan, decreased plasma norepinephrine concentrations, LF/HF-HRV, and LF-SBPV in patients with MetS. Furthermore, although both telmisartan and candesartan improved the impaired BRS, the improvement of the impaired BRS was significantly greater in the telmisartan-treated group than in the candesartan-treated group. BRS might be improved because of the reduction in blood pressure [39]. In the present study, however, telmisartan and candesartan caused similar depressor effects. We also demonstrated that decreases in forearm vascular resistance were significantly positively correlated with decreases in plasma norepinephrine concentrations and the increases in BRS. In the present study, we did not address the mechanisms by which telmisartan inhibits SNS activation and improves baroreflex dysfunction to a greater extent than candesartan in patients with MetS. We previously

demonstrated, however, that telmisartan inhibits SNS activation in hypertensive rats [40]. Interestingly, a previous study found that telmisartan can penetrate the blood–brain barrier in both a dose and time-dependent manner to inhibit the centrally mediated effects of angiotensin II following peripheral administration [41]. We demonstrated that oxidative stress in the cardiovascular center of the brainstem causes sympatho-excitation and baroreflex dysfunction [42,43]. In the brain, oxidative stress is mainly produced by the activation of angiotensin II type 1 receptors [44,45]. Taken together, these findings lead us to speculate that oral administration of telmisartan, but not candesartan, improves the impaired BRS and SNS activation due to a reduction in the oxidative stress in the brain. Furthermore, this sympatho-inhibitory effect of telmisartan might, at least in part, induce the amelioration of endothelial dysfunction in patients with MetS.

Telmisartan also reduces serum uric acid in patients with MetS. Serum uric acid levels are increased in patients with MetS because insulin increases both sodium and uric acid reabsorption [46,47]. Furthermore, elevated serum uric acid levels appear to be associated with endothelial dysfunction [46,47] and may have a role in the increased vascular risk of patients with MetS [47]. On the basis of the results of the present study, we speculate that telmisartan reduces serum uric acid through its effects to improve insulin resistance.

In the present study, we did not address the role of leptin in the regulation of SNS in patients with MetS. Leptin is an adipocyte-derived hormone that has a key role in the regulation of body weight through its actions on appetite and metabolism in addition to increasing blood pressure and SNS activation [48]. Rahmouni *et al.* [48] suggested that mice with diet-induced obesity exhibit circulating hyperleptinemia and resistance to the metabolic actions of leptin. In the present study, although we did not measure leptin levels, it is possible that the different effects of the ARBs on activation of the SNS and the endothelial dysfunction are due to their different effects on leptins.

The increasing number of patients with MetS is a worldwide health problem because patients with MetS are considered to be at a high risk for cardiovascular disease. Renin–angiotensin system inhibitors are preferred for patients with MetS [23,24]. Important targets of treatments for cardiovascular disease include endothelial and autonomic dysfunction. In the present study we demonstrated that ARBs improve endothelial dysfunction in resistance arteries and autonomic dysfunction in patients with MetS. Furthermore, amelioration of endothelial and autonomic dysfunction in patients with MetS was significantly greater in the telmisartan-treated group than in the candesartan-treated group, despite the similar depressor effects of the two drugs. These findings suggest that telmisartan has a unique multitherapeutic potential for hypertension, insulin resistance, endothelial dysfunction, and autonomic dysfunction in patients with MetS and that these beneficial effects are not class effects of ARBs.

The present study has some limitations. First, the present study has a small sample size. To strengthen the results of the present study, another clinical study should be performed with a larger sample size and longer follow-up period. Second, four or five patients in each group were treated with amlodipine, which might affect endothelial function [49]. However, the patients had been taking amlodipine for more than a year. They still showed high blood pressure and metabolic profile. Therefore, we enrolled the patients in the present study. We found that they showed endothelial dysfunction compared with other patients. Third, the effects of individual nutritional education were not quantified in the present study. The differences in daily nutrition may not be small, even if all the patients enrolled in the present study received individual nutritional education. Fourth, plasma norepinephrine concentration is a variable marker, and is changed by many factors [50]. Spectral analysis of blood pressure and heart rate variability is also not considered to be a reliable marker of SNS activity [50]. Therefore, it remains to be determined whether oral-administered telmisartan has a definitive sympatho-inhibitory effect in patients with MetS by directly assessing SNS activity using the norepinephrine radiolabeled spillover technique or microneurographic recordings of efferent postganglionic muscle sympathetic nerve firing rates. Spectral analysis of blood pressure and heart rate has also been suggested to function as a relatively 'direct' assessment of SNS activity [30]. The effects of telmisartan on the plasma norepinephrine concentrations, LF/HF-HRV, and LF-SBPV in the present study indicate that this drug has sympatho-inhibitory effects.

In conclusion, in patients with MetS, ARBs ameliorated endothelial dysfunction. The improvement in the endothelial function was significantly greater in the telmisartan-treated group than in the candesartan-treated group, despite the similar depressor effects of the two drugs. Furthermore, telmisartan, but not candesartan, inhibited SNS activity in patients with MetS. Telmisartan improved BRS to a greater extent than did candesartan. These findings suggest that ARBs have beneficial effects on endothelial dysfunction, baroreflex dysfunction, and sympathetic hyperactivity in patients with MetS, and that these effects of ARBs are not class effects.

ACKNOWLEDGEMENTS

The study was supported by a Grant-in-Aid for Scientific Research from the Japan Society for the Promotion of Science (B193290231) and in part by a Kimura Memorial Foundation Research Grant.

Conflicts of interest

There are no conflicts of interest.

REFERENCES

1. Grundy SM, Cleeman JI, Daniels SR, Donato KA, Eckel RH, Franklin BA, *et al.* Diagnosis and management of the metabolic syndrome: an American Heart Association/National Heart, Lung, and Blood Institute Scientific Statement. *Circulation* 2005; 112:2735–2752.
2. Grundy SM. Metabolic syndrome pandemic. *Arterioscler Thromb Vasc Biol* 2008; 28:629–636.
3. Gami AS, Witt BJ, Howard DE, Erwin PJ, Gami LA, Somers VK, Montori VM. Metabolic syndrome and risk of incident cardiovascular events and death: a systematic review and meta-analysis of longitudinal studies. *J Am Coll Cardiol* 2007; 49:403–414.

4. Hamburg NM, Larson MG, Vita JA, Vasan RS, Keyes MJ, Widlansky ME, *et al.* Metabolic syndrome, insulin resistance, and brachial artery vasodilator function in Framingham Offspring participants without clinical evidence of cardiovascular disease. *Am J Cardiol* 2008; 101:82–88.
5. Bahia L, Aguiar LG, Villela N, Bottino D, Godoy-Matos AF, Geloneze B, *et al.* Adiponectin is associated with improvement of endothelial function after rosiglitazone treatment in nondiabetic individuals with metabolic syndrome. *Atherosclerosis* 2007; 195:138–146.
6. Lind L. Endothelium-dependent vasodilation, insulin resistance and the metabolic syndrome in an elderly cohort: the Prospective Investigation of the Vasculature in Uppsala Seniors (PIVUS) study. *Atherosclerosis* 2008; 196:795–802.
7. Ross R. Atherosclerosis-an inflammatory disease. *N Engl J Med* 1999; 340:115–126.
8. Perticone F, Ceravolo R, Pujia A, Ventura G, Iacopino S, Scozzafava A, *et al.* Prognostic significance of endothelial dysfunction in hypertensive patients. *Circulation* 2001; 104:191–196.
9. Fathi R, Haluska B, Isbel N, Short L, Marwick TH. The relative importance of vascular structure and function in predicting cardiovascular events. *J Am Coll Cardiol* 2004; 43:616–623.
10. Frick M, Suessenbacher A, Alber HF, Dichtl W, Ulmer H, Pachinger O, Weidinger F. Prognostic value of brachial artery endothelial function and wall thickness. *J Am Coll Cardiol* 2005; 46:1006–1010.
11. Kullo IJ, Malik AR. Arterial ultrasonography and tonometry as adjuncts to cardiovascular risk stratification. *J Am Coll Cardiol* 2007; 49:1413–1426.
12. Title LM, Lonn E, Charbonneau F, Fung M, Mather KJ, Verma S, Anderson TJ. Relationship between brachial artery flow-mediated dilatation, hyperemic shear stress, and the metabolic syndrome. *Vasc Med* 2008; 13:263–270.
13. Wu HD, Katz SD, Beniaminovitz A, Khan T, DiTullio MR, Homma S. Assessment of endothelium-mediated vasodilation of the peripheral circulation by transcutaneous ultrasonography and venous occlusion plethysmography. *Heart Vessels* 1999; 14:143–148.
14. Egashira K, Suzuki S, Hirooka Y, Kai H, Sugimachi M, Imaizumi T, Takeshita A. Impaired endothelium-dependent vasodilation of large epicardial and resistance coronary arteries in patients with essential hypertension. Different responses to acetylcholine and substance P. *Hypertension* 1995; 25:201–206.
15. Lind L, Berglund L, Larson A, Sundstrom J. Endothelial function in resistance and conduit arteries and 5-year risk of cardiovascular disease. *Circulation* 2011; 123:1545–1551.
16. Grassi G, Arenare F, Quarti-Trevano F, Seravalle G, Mancia G. Heart rate, sympathetic cardiovascular influences, and the metabolic syndrome. *Prog Cardiovasc Dis* 2009; 52:31–38.
17. Grassi G, Dell'Oro R, Quarti-Trevano F, Scopelliti F, Seravalle G, Paleari F, *et al.* Neuroadrenergic and reflex abnormalities in patients with metabolic syndrome. *Diabetologia* 2005; 48:1359–1365.
18. Mancia G, Bousquet P, Elghozi JL, Esler M, Grassi G, Julius S, *et al.* The sympathetic nervous system and the metabolic syndrome. *J Hypertens* 2007; 25:909–920.
19. Landsberg L. Insulin-mediated sympathetic stimulation: role in the pathogenesis of obesity-related hypertension (or, how insulin affects blood pressure, and why). *J Hypertens* 2001; 19:523–528.
20. Lee ZS, Critchley JA, Tomlinson B, Young RP, Thomas GN, Corkram CS, *et al.* Urinary epinephrine and norepinephrine interrelations with obesity, insulin, and the metabolic syndrome in Hong Kong Chinese. *Metabolism* 2001; 50:135–143.
21. Hijmering ML, Stroes ES, Olijhoek J, Hutten BA, Blankestijn PJ, Rabelink TJ. Sympathetic activation markedly reduces endothelium-dependent, flow-mediated vasodilation. *J Am Coll Cardiol* 2002; 39:683–688.
22. Lindgren K, Hagelin E, Hansén N, Lind L. Baroreceptor sensitivity is impaired in elderly subjects with metabolic syndrome and insulin resistance. *J Hypertens* 2006; 24:143–150.
23. Elliott WJ, Meyer PM. Incident diabetes in clinical trials of antihypertensive drugs: a network meta-analysis. *Lancet* 2007; 369:201–207.
24. Ogihara T, Kikuchi K, Matsuoka H, Fujita T, Higaki J, Horiuchi M, *et al.* The Japanese Society of Hypertension Guidelines for the Management of Hypertension (JSH 2009). *Hypertens Res* 2009; 32:3–107.
25. Hirooka Y, Imaizumi T, Tagawa T, Shiramoto M, Endo T, Ando S, Takeshita A. Effects of L-arginine on impaired acetylcholine-induced and ischemic vasodilation of the forearm in patients with heart failure. *Circulation* 1994; 90:658–668.
26. Hirooka Y, Eshima K, Setoguchi S, Kishi T, Egashira K, Takeshita A. Vitamin C improves attenuated angiotensin II-induced endothelium-dependent vasodilation in human forearm vessels. *Hypertens Res* 2003; 26:953–959.
27. Kishi T, Hirooka Y, Masumoto A, Ito K, Kimura Y, Inokuchi K, *et al.* Rho-kinase inhibitor improves increased vascular resistance and impaired vasodilation of forearm in patients with heart failure. *Circulation* 2005; 111:2741–2747.
28. Oda E, Watanabe K. Japanese criteria of metabolic syndrome. *Circ J* 2006; 70:364.
29. Hilz MJ, Marthol H, Schwab S, Kolodny EH, Brys M, Stemper B. Enzyme replacement therapy improves cardiovascular responses to orthostatic challenge in Fabry patients. *J Hypertens* 2010; 28:1438–1448.
30. Grassi G. Assessment of sympathetic cardiovascular drive in human hypertension: achievements and perspectives. *Hypertension* 2009; 54:690–697.
31. Parati G, Di Rienzo M, Bertinieri G, Pomidossi G, Casadei R, Groppelli A, *et al.* Evaluation of the baroreceptor-heart rate reflex by 24-h intra-arterial blood pressure monitoring in humans. *Hypertension* 1988; 12:214–222.
32. Heusser K, Tank J, Engeli S, Diedrich A, Menne J, Eckert S, *et al.* Carotid baroreceptor stimulation, sympathetic activity, baroreflex function, and blood pressure in hypertensive patients. *Hypertension* 2010; 55:619–626.
33. Kataoka H, Murakami R, Numaguchi Y, Okumura K, Murohara T. Angiotensin II type 1 receptor blockers prevent tumor necrosis factor-á-mediated endothelial nitric oxide synthase reduction and superoxide production in human umbilical vein endothelial cells. *Eur J Pharmacol* 2010; 636:36–41.
34. Psherer S, Heemann U, Frank H. Effect of renin-angiotensin system blockade on insulin resistance and inflammatory parameters in patients with impaired glucose tolerance. *Diabetes Care* 2010; 33:914–919.
35. Toyama K, Nakamura T, Kataoka K, Yasuda O, Fukuda M, Tokutomi Y, *et al.* Telmisartan protects against diabetic vascular complications in a mouse model of obesity and type 2 diabetes, partially through peroxisome proliferator activated receptor-ã-dependent activity. *Biochem Biophys Res Commun* 2011; 410:508–513.
36. Yoshida T, Yamagishi S, Nakamura K, Matsui T, Imaizumi T, Takeuchi M, *et al.* Telmisartan inhibits AGE-induced C-reactive protein production through downregulation of the receptor for AGE via peroxisome proliferator-activated receptor-gamma activation. *Diabetologia* 2008; 49:3094–3098.
37. Ouchi N, Ohishi M, Kihara S, Funahashi T, Nakamura T, Nagaretani H, *et al.* Association of hypoadiponectinemia with impaired vasoreactivity. *Hypertension* 2003; 42:231–234.
38. Shimabukuro M, Higa N, Asahi T, Oshiro Y, Takasu N, Tagawa T, *et al.* Hypoadiponectinemia is closely linked to endothelial dysfunction in man. *J Clin Endocrinol Metab* 2003; 88:3236–3240.
39. Persson PB. Baroreflex in hypertension: a mystery revisited. *Hypertension* 2005; 46:1095–1096.
40. Hirooka Y, Sagara Y, Kishi T, Sunagawa K. Oxidative stress and central cardiovascular regulation. Pathogenesis of hypertension and therapeutic aspects. *Circ J* 2010; 74:827–835.
41. Gohlke P, Weiss S, Jansen A, Wienen W, Stangier J, Rascher W, *et al.* AT1 receptor antagonist telmisartan administered peripherally inhibits central responses to angiotensin II in conscious rats. *J Pharmacol Exp Ther* 2001; 298:62–70.
42. Kishi T, Hirooka Y, Kimura Y, Ito K, Shimokawa H, Takeshita A. Increased reactive oxygen species in rostral ventrolateral medulla contribute to neural mechanisms of hypertension in stroke-prone spontaneously hypertensive rats. *Circulation* 2004; 109:2357–2362.
43. Kishi T, Hirooka Y, Shimokawa H, Takeshita A, Sunagawa K. Atorvastatin reduces oxidative stress in the rostral ventrolateral medulla of stroke-prone spontaneously hypertensive rats. *Clin Exp Hypertens* 2008; 30:3–11.
44. Nozoe M, Hirooka Y, Koga Y, Araki S, Konno S, Kishi T, *et al.* Mitochondria-derived reactive oxygen species mediate sympathoexcitation induced by angiotensin II in the rostral ventrolateral medulla. *J Hypertens* 2008; 26:2176–2184.
45. Kishi T, Hirooka Y, Konno S, Ogawa K, Sunagawa K. Angiotensin II type 1 receptor-activated caspase-3 through ras/mitogen-activated protein kinase/extracellular signal-regulated kinase in the rostral

ventrolateral medulla is involved in sympathoexcitation in stroke-prone spontaneously hypertensive rats. *Hypertension* 2010; 55:291–297.
46. Zoccali C, Maio R, Mallamaci F, Sesti G, Perticone F. Uric acid and endothelial dysfunction in essential hypertension. *J Am Soc Nephrol* 2006; 17:1466–1471.
47. Tsouli SG, Liberopoulos EN, Mikhailidis DP, Athyros VG, Elisaf MS. Elevated serum uric acid levels in metabolic syndrome: an active component or an innocent bystander? *Metabolism* 2006; 55:1293–1301.
48. Rahmouni K, Morgan DA, Morgan GM, Mark AL, Haynes WG. Role of selective leptin resistance in diet-induced obesity hypertension. *Diabetes* 2005; 54:2012–2018.
49. Virdis A, Ghiadoni L, Taddei S. Effects of antihypertensive treatment on endothelial function. *Curr Hypertens Rep* 2011; 13:276–281.
50. Triposkiadis F, Karayannis G, Giamouzis G, Skoularigis J, Louridas G, Butler J. The sympathetic nervous system in heart failure: physiology, pathophysiology, and clinical implications. *J Am Coll Cardiol* 2009; 54:1747–1762.

Reviewers' Summary Evaluations

Reviewer 2

This paper showed that ARBs improved endothelial and baroreflex function in a small cohort of patients with metabolic syndrome. Better results were obtained with the ARB telmisartan, particularly with respect to the reduction of sympathetic hyperactivity. This paper further extends the knowledge on the cardiovascular protective role of ARBs in dysmetabolic patients. However the mechanism involved in different effects induced by individual ARBs is not addressed in this paper.

Reviewer 3

This work investigates the effects of two Angiotensin Receptor Blockers (ARBs) – candesartan and telmisartan – on endothelial and autonomic dysfunction in Japanese patients with metabolic syndrome (MetS). The authors have found that both candesartan and telmisartan improve endothelial function in MetS patients even if telmisartan performs better. Moreover, they have found that telmisartan, but not candesartan, significantly improves baroreflex dysfunction and reduces plasma norepinephrine concentration in MetS patients. Despite previous manuscripts already focused on role of ARBs in endothelial dysfunction in MetS. (i.e. Irbesartan: Sola *et al.* Circulation 2005), this works compared the effects of two different ARBs (telmisartan and candesartan) and therefore provides additional and original information.

Mitochondrion 12 (2012) 449–458

Contents lists available at SciVerse ScienceDirect

Mitochondrion

journal homepage: www.elsevier.com/locate/mito

Recombinant mitochondrial transcription factor A protein inhibits nuclear factor of activated T cells signaling and attenuates pathological hypertrophy of cardiac myocytes

Takeo Fujino [a], Tomomi Ide [a,*], Masayoshi Yoshida [a], Ken Onitsuka [a], Atsushi Tanaka [a], Yuko Hata [a], Motohiro Nishida [b], Takako Takehara [a], Takaaki Kanemaru [c], Naoyuki Kitajima [b], Shinya Takazaki [d], Hitoshi Kurose [b], Dongchon Kang [d], Kenji Sunagawa [a]

[a] Department of Cardiovascular Medicine, Graduate School of Medical Sciences, Kyushu University, 3-1-1, Maidashi, Higashi-ku, Fukuoka 812-8582, Japan
[b] Department of Pharmacology and Toxicology, Graduate School of Pharmaceutical Sciences, Kyushu University, 3-1-1, Maidashi, Higashi-ku, Fukuoka 812-8582, Japan
[c] Morphology and Core Unit, Kyushu University Hospital, 3-1-1, Maidashi, Higashi-ku, Fukuoka 812-8582, Japan
[d] Department of Clinical Chemistry and Laboratory Medicine, Graduate School of Medical Sciences, Kyushu University, 3-1-1, Maidashi, Higashi-ku, Fukuoka 812-8582, Japan

ARTICLE INFO

Article history:
Received 27 March 2012
Received in revised form 6 June 2012
Accepted 11 June 2012
Available online 16 June 2012

Keywords:
Cardiac hypertrophy
Mitochondrial transcription factor A
Nuclear factor of activated T cells

ABSTRACT

The overexpression of mitochondrial transcription factor A (TFAM) attenuates the decrease in mtDNA copy number after myocardial infarction, ameliorates pathological hypertrophy, and markedly improves survival. However, non-transgenic strategy to increase mtDNA for the treatment of pathological hypertrophy remains unknown. We produced recombinant human TFAM protein (rhTFAM). rhTFAM rapidly entered into mitochondria of cultured cardiac myocytes. rhTFAM increased mtDNA and abolished the activation of nuclear factor of activated T cells (NFAT), which is well known to activate pathological hypertrophy. rhTFAM attenuated subsequent morphological hypertrophy of myocytes as well. rhTFAM would be an attractive molecule in attenuating cardiac pathological hypertrophy.

1. Introduction

Mitochondrial dysfunction has been reported in various forms of heart failure. Mitochondrial DNA (mtDNA) is decreased in the heart from post-myocardial infarction (MI) model in mice (Ide et al., 2001). In human as well, Karamanlidis et al. demonstrated that mitochondrial biogenesis is severely impaired in the myocardium from end-stage heart failure patients. They also showed that there was no significant change in the expression of the fibroblast marker in their sample, suggesting the decrease of mtDNA and mitochondrial biogenesis are not due to the fibrosis occurring under these conditions, changing the ratio of cardiac myocytes with a high amount of mitochondria to fibroblasts and other cell types with low amounts (Karamanlidis et al., 2010). mtDNA could be a major target for locally generated reactive oxygen species (ROS), and an intimate link among mtDNA damage and defects in the electron transport function might play an important role in the development and progression of cardiac remodeling and failure (Ide et al., 2001).

Mitochondrial transcription factor A (TFAM), a nucleus-encoded protein, binding upstream of the light strand and heavy strand promoters of mtDNA, promotes transcription of mtDNA. It also plays an important role in regulating mtDNA copy number (Kanki et al., 2004). TFAM is a high mobility group protein having DNA-binding properties, regardless of its DNA sequence (Parisi and Clayton, 1991). TFAM molecules are abundant enough to cover the entire mtDNA, and indeed most of them bind mtDNA, suggesting that mtDNA is packaged with TFAM (Alam et al., 2003; Kang et al., 2007). Disruption of the *tfam* gene in mice has been shown to cause depletion of mtDNA, loss of mitochondrial transcripts, loss of mtDNA-encoded polypeptides, and severe respiratory chain deficiency (Larsson et al., 1998). Moreover, targeted disruption of *tfam* in cardiac myocytes induced deletion of mtDNA and dilated cardiomyopathy (Li et al., 2000; Wang et al., 1999). In addition, a reduction in TFAM expression has been demonstrated in several forms of cardiac failure (Garnier et al., 2003; Ide et al., 2001; Karamanlidis et al., 2010). We have previously demonstrated in mice, in MI, that TFAM

Abbreviations: mtDNA, mitochondrial DNA; ROS, reactive oxygen species; TFAM, mitochondrial transcription factor A; MI, myocardial infarction; NFAT, nuclear factor of activated T cells; GST, glutathione S-transferase; MTS, mitochondrial targeting signal; rhTFAM, recombinant human TFAM; ΔMTS-rhTFAM, rhTFAM without MTS; rhTFAM-ΔC, rhTFAM lacking C-terminal tail; MAPK, mitogen-activated protein kinase; ERK, extracellular signal-regulated kinase; COX I, cytochrome c oxidase I; COX III, cytochrome c oxidase III; SDHA, succinate dehydrogenase complex subunit A; NDUFA9, NADH dehydrogenase 1 alpha subcomplex subunit 9; ATIII, antithrombin III; RPL27, ribosomal protein L27; MCIP1, modulatory calcineurin interacting protein 1; HPRT, hypoxanthine guanine phosphoribosyl transferase; AngII, angiotensin II; ET-1, endothelin-1; BNP, brain natriuretic peptide.

* Corresponding author. Tel.: +81 92 642 5360; fax: +81 92 642 5374.
E-mail address: tomomi_i@cardiol.med.kyushu-u.ac.jp (T. Ide).

1567-7249/$ – see front matter © 2012 Elsevier B.V. and Mitochondria Research Society. All rights reserved.
doi:10.1016/j.mito.2012.06.002

overexpression attenuated the decrease in mtDNA copy number, ameliorated pathological hypertrophy, and dramatically improved survival rate (Ikeuchi et al., 2005). In addition, the overexpression of TFAM in Hela cells reduced mitochondrial ROS generation (Hayashi et al., 2008). Taken together, these findings indicate that upregulating TFAM results in increasing mtDNA copy number and attenuates cardiac pathological hypertrophy. However, the effective way how to increase TFAM expression or mtDNA copy number in clinical situation remains unknown.

Recent study showed that exogenously administered recombinant TFAM engineered with an N-terminal protein transduction domain, followed by a matrix mitochondrial localization sequence, was recruited into mitochondria of cultured cells (Iyer et al., 2009). Therefore it is conceivable that exogenously administered recombinant TFAM manifests beneficial impacts on myocytes, and this method could be useful for the therapy of cardiac pathological hypertrophy. In the present study, we examined whether exogenous recombinant TFAM protein was recruited into cardiac myocytes and functioned to increase mtDNA copy number and attenuate hypertrophy of myocytes in vitro. The results indicated that recombinant TFAM protein inhibited nuclear factor of activated T cells (NFAT) signaling and prevented pathological hypertrophy of cardiac myocytes.

2. Material and methods

2.1. Preparation of human TFAM protein

We used a glutathione S-transferase (GST) gene fusion purification protocol to synthesize recombinant human TFAM protein. Two TFAM proteins, rhTFAM (recombinant human TFAM with mitochondrial targeting signal (MTS)) and ΔMTS-rhTFAM (recombinant human TFAM without MTS), were prepared. The nucleotide sequences corresponding to human TFAM and TFAM without MTS were cloned from human cDNA library, and were subcloned into pGEX-6P-1 (GE Healthcare). The constructs were transformed into competent cells (BL21 (DE3), Invitrogen). The transformed bacteria were cultured in LB medium (MP Biochemicals) supplemented with 100 μg/ml ampicillin (Wako), in the shaking incubator (Bio-Shaker BR-300LF, TAITEC). When the culture achieved an optical density of wavelength 600 nm to 0.5–0.7, isopropyl-β-D-thiogalactopyranoside (0.7 mM, nacalai tesque) was added to the medium and incubated for further 2 h. Growth and expression of the bacteria culture were performed at 37 °C with variable agitation and airflow. The bacteria were harvested and pelleted by centrifugation at 8000*g* and stored at −80 °C.

Cell pellets were resuspended in sonication buffer (20 mM Tris–HCl, 500 mM NaCl, 250 mM, 2-mercaptoethanol 5 mM, 1% NP-40 and protease inhibitor cocktail (Complete Mini, Roche Diagnostics)) and mildly sonicated at 4 °C. The lysate was then clarified by centrifugation at 8000*g* for 30 min. The supernatant was mixed with Glutathione Sepharose 4B resin (GE Healthcare) for 2 h and applied to polypropylene columns (Thermo SCIENTIFIC). Resin absorbed with GST-TFAM protein was washed with wash buffer (20 mM Tris–HCl, 150 mM NaCl, 5 mM 2-mercaptoethanol, 0.1% NP-40) to isolate the vector protein. Then it was mixed with Turbo3C Protease (160 units/ml, Accelagen) and elusion buffer (20 mM Tris–HCl, 150 mM NaCl, 5 M 2-mercaptoethanol, 0.1% NP-40) at 4 °C overnight to remove GST from TFAM. The flow-through was collected and dialyzed with Slide-a-lyzer Dialysis Cassette (7 K MWCO, Thermo Scientific) in phosphate buffered saline (PBS). The solution was screened via sodium dodecyl sulfate (SDS)–polyacrylamide gel electrophoresis (PAGE) analysis for proper size and purity. The purity was above 98% by Coomassie Brilliant Blue (CBB) staining. Western blot analysis was also performed using anti-human TFAM specific antibody to verify the success of target protein purification (Fig. 1). The solution was stored at −80 °C and used as recombinant TFAM protein. We also performed the same procedure using empty vector without TFAM sequence and the product was also stored at −80 °C. In addition, we synthesized recombinant human TFAM lacking the C-terminal 25

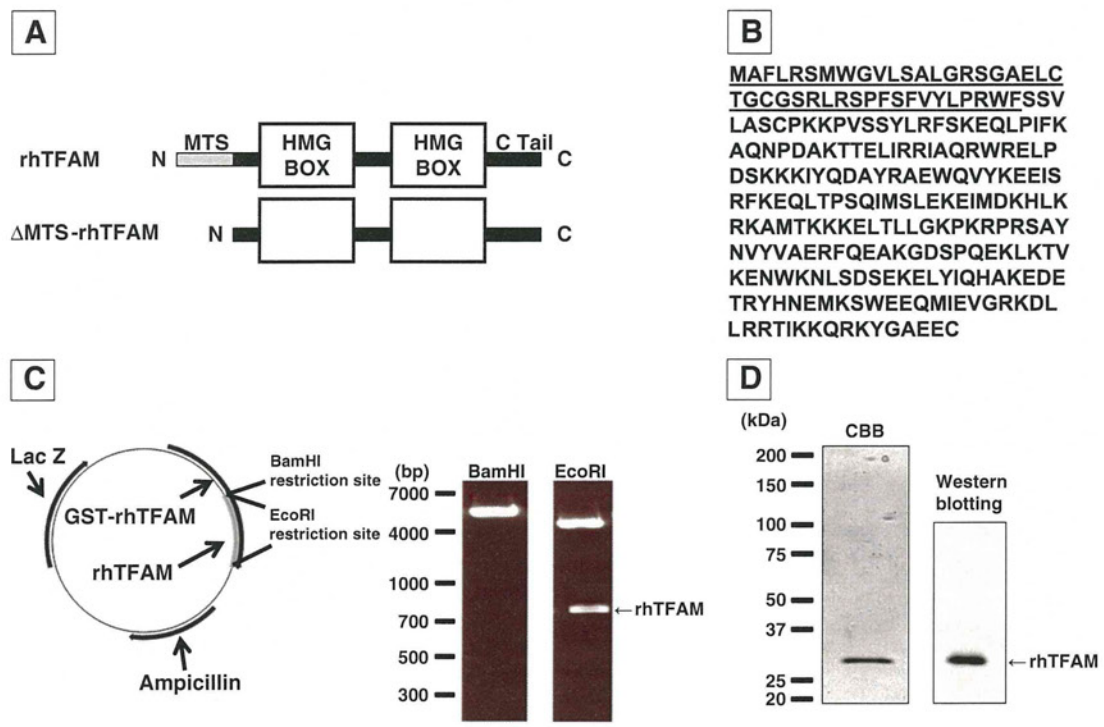

Fig. 1. Synthesis of recombinant human TFAM protein. (A and B) Schematic structure (A) and amino acid sequence (B) of human TFAM protein. Underlined part is MTS. (C) Schematic structure and electrophoresis of pGEX-6P-1-TFAM, the subcloned plasmid we constructed for synthesizing recombinant TFAM. TFAM sequence was inserted between the EcoRI restriction sites. The left lane shows linear whole plasmid (BamHI restriction), and the right lane shows electrophoretically separated pGEX-6P-1 and TFAM (EcoRI restriction). (D) SDS-PAGE analysis of the product. We confirmed the product as TFAM by CBB staining (left lane) and Western blotting using human TFAM -specific antibody (right lane).

amino acids (rhTFAM-ΔC) as described previously (Ohgaki et al., 2007).

2.2. Preparation and culture of cardiac myocytes and RAW 264.7 cells

All procedures and animal care were approved by the Committee on Ethics of Animal Experiment, Kyushu University Graduate School of Medical and Pharmaceutical Sciences and performed in accordance with the Guideline for Animal Experiment of Kyushu University, and the Guide for the Care and Use of Laboratory Animals published by the US National Institutes of Health (NIH Publication No. 85–23, revised 1996). Primary culture of neonatal rat ventricular myocytes was prepared from the ventricles of neonatal SD rats as described previously (Tsutsumi et al., 2008). Neonatal rats were euthanized by decapitation under anaesthesia with isoflurane, after which the hearts were rapidly excised and digested. Anaesthesia depth was monitored by limb withdrawal using toe pinching. After digestion of the myocardial tissue with trypsin (Wako) and collagenase type 2 (Worthington), cells were suspended in Dulbecco's Modified Eagle's Medium (Sigma-Aldrich) containing 10% fetal bovine serum (FBS, Thermo Scientific), penicillin (Invitrogen) and streptomycin (Invitrogen), and plated twice in 100 mm culture dishes (Cellstar, greiner bio-one) for 70 min each to reduce the number of non-myocytes. Non-adherent cells were plated in culture dishes (Primaria, Falcon) at an appropriate density for each experiment. Myocytes were maintained at 37 °C in humidified air with 5% CO_2 for 36 h after the plating to the culture dishes. The culture medium was changed and rhTFAM protein was added to the medium 12 h before each experiment.

RAW 264.7 cells, mouse leukemic monocyte macrophage cell line, were originally obtained from American Type Culture Collection (ATCC; cat.no.TIB-71).

2.3. Western blot analyses

Western blot analysis of cardiac myocytes was performed as described previously (Kanki et al., 2004). Cells were carefully washed with Hanks' balanced salt solution (HBSS, Invitrogen) and collected in lysis buffer (RIPA Buffer, Thermo Scientific) with protease inhibitor cocktail. Equal amounts of protein (10 μg protein per lane), estimated by the bicinchoninic acid assay with the use of BCA Protein Assay (Thermo Scientific), were separated on SDS-PAGE and then electrophoretically transferred to a nitrocellulose membrane (Trans-Blot, Bio-Rad). After blocking for 2 h, the membrane was incubated with a certain primary antibody at 4 °C overnight. Then they were incubated with corresponding secondary antibody for 1 h at room temperature. The chemiluminescence was detected with an ECL™ Western Blotting Detection Reagents (GE Healthcare) according to the manufacturer's recommendation. The signal was visualized and recorded with a chilled charge-coupled device camera, LAS3000 (FUJIFILM). We also performed the same procedure using RAW 264.7 cells.

Antibody to human TFAM was produced by immunizing rabbits with recombinant human TFAM. Antibodies to cytochrome c oxidase I (COX I), cytochrome c oxidase III (COX III), succinate dehydrogenase complex subunit A (SDHA), and NADH dehydrogenase 1 alpha subcomplex subunit 9 (NDUFA9) were from Invitrogen. Antibody to glyceraldehyde 3-phosphate dehydrogenase (GAPDH) and secondary antibodies for Western blotting were obtained from Santa Cruz Biotechnology. Densities of the immunoreactive bands were evaluated using NIH ImageJ software, and relative amounts were quantified relative to GAPDH.

For the measurement of mitogen-activated protein kinase (MAPK) p44/42 (extracellular signal-regulated kinase (ERK) 1/2)) phosphorylation, cells were stimulated with endothelin-1 (ET-1, 100 nM, Sigma-Aldrich) for 30 min and collected. Antibodies to phospho-MAPK p44/42 and total-MAPK p44/42 were from Invitrogen. Total-MAPK p44/42 protein contents were also determined after stripping the phosphoblots with stripping solution (nacalai tesque) in order to verify for protein loading. Signal intensities were quantified as the ratio of phospho- to total-MAPK p44/42.

2.4. Immunostaining

Cells were washed with HBSS and treated with 500 nM MitoTracker Orange (Invitrogen) in culture medium for 15 min. They were again washed with HBSS and fixed with −20 °C methanol for 20 min. After blocking with the mixture of 10% FBS and 1% bovine serum albumin (Wako), they were incubated with anti-human TFAM antibody at 4 °C overnight. Then they were incubated with fluorescence-labeled secondary antibody (Alexa Fluor 488 chicken anti-rabbit IgG, Invitrogen) for 1 h. They were mounted with mounting medium with DAPI (Vectashield, Vector Laboratories) and observed by confocal microscopy (A1, Nikon).

2.5. Cell viability

Cell viability was measured using Cell Counting Kit-8 (Dojindo) as manufacturer's protocol. Briefly, the reagent was added to the culture medium and incubated for 3 h. Then the absorbance of the culture medium at 450 nm was measured by the microplate reader (Infinite 200, TECAN).

2.6. Lactate dehydrogenase (LDH) Assay

LDH concentration in the culture medium was measured using LDH-Cytotoxicity Assay Kit (Wako) as manufacturer's protocol. Briefly, the culture medium was reacted with the reagent for 30 min at room temperature. Then the absorbance at 560 nm was measured by the microplate reader.

2.7. Observation by transmission electron microscopy (TEM)

Cardiac myocytes were collected and fixed with 2% glutaraldehyde (TAAB), post-fixed in 1% osmium tetroxide, and embedded. Ultrathin sections were post-stained with Sato's lead staining solution and observed with TEM (H7000E, Hitachi).

2.8. Real-time polymerase chain reaction (PCR) analyses

mtDNA copy number and mRNA expression were quantified by real-time PCR analysis, as described previously (Kanki et al., 2004; Lagouge et al., 2006). Total DNA was extracted with DNeasy tissue kit (Qiagen), and total RNA was extracted with RNeasy tissue kit (Qiagen). The total DNA or RNA was quantified by absorbance method (BioPhotometer, Eppendorf).

Total DNA was treated with BamHI (Takara) for 6 h and the relative amount of mtDNA was quantified by quantitative PCR. The PCR mixture contained 3 ng of the total DNA, 12 pmol each of primers (5′-ACTCCCTATTCGGAGCCCTA-3′ and 5′-GGAGCTCGATTTGTTTCTGC-3′ for mtDNA) in 30 μl. To estimate the amount of genomic DNA as an internal standard, antithrombin III (ATIII) gene was amplified in a 30 μl reaction mixture containing 3 ng of the total DNA, 12 pmol each of primers (5′-TGCTACTCATTGGTGCCTTG-3′ and 5′-TTCCGGAACCTTCTGCTCTA-3′). The amount of mtDNA was adjusted to the amount of genomic DNA. All reactions were performed with SYBR Premix Ex Taq II (Takara) and Applied Biosystems 7500 Real-Time PCR system (Applied Biosystems) according to the manufacture's protocol. We also confirmed the result using another primer set for mtDNA (5′-CCCAGCCACCACTATCATTC-3′ and 5′-TGATGTTGGGGTTATGTTGG-3′). We also performed the same procedure using RAW 264.7 cells, using the primer set for mtDNA (5′-TGTAAGCCGGACTGCTAATG-3′ and 3′-AGCTGGAGCCGTAATTACAG-5′)

and for ribosomal protein L27 (RPL27, 5′-CCTCATGCCCACAAGGTACTC-3′ and 3′-TCGCTCCTCAAACTTGACC-5′) as an internal standard.

Total RNA was incubated with DNase I for 30 min and reverse transcription was performed with ReverTra Ace qPCR RT Kit (Toyobo). The relative amount of modulatory calcineurin interacting protein 1 (MCIP1) cDNA was quantified using in the same way as quantification of mtDNA copy number, using the PCR mixture contained 5 ng of the total cDNA, 12 pmol each of primers (5′-TTGGGAACTGTTGGTTGACA-3′ and 5′-ATGGCTACGGCATACTCCAC-3′ for MCIP1) in 30 μl.

In in vivo experiments, 8- to 10-week-old male TFAM overexpression mice and their littermates were used. Under anaesthesia with pentobarbital sodium (30 mg/g BW, i.p.), the hearts were excised and RNA was extracted with RNeasy tissue kit. After reverse transcription, the relative amount of cDNA was quantified using the PCR mixture contained 5 ng of the total cDNA, 12 pmol each of primers (5′-CCGTGTGGAATTGTCCTTCTC-3′ and 5′-GACCCCATGTGCAGAGAAAAC-3′ for MCIP1) in 30 μl. We used hypoxanthine guanine phosphoribosyl transferase (HPRT) gene as an internal standard (5′-CTGGTGAAAAG GACCTCTCG-3′ and 5′-AACTTGCGCTCATCTTAGGC-3′).

2.9. Nuclear translocation of NFAT

In order to assess nuclear translocation of NFAT, production and infection of recombinant adenovirus including green fluorescent protein (GFP)-fused N-terminal region of NFAT4 (we referred as just NFAT in this article) were performed as described previously (Fujii et al., 2005; Nishida et al., 2007). Cardiac myocytes were infected with the adenovirus at a multiplicity of infection of 300 for 60 h. After the stimulation for 30 min with angiotensin II (AngII, 100 nM, Sigma-Aldrich) or ET-1 (100 nM), cells were fixed by 10% formaldehyde (Sigma-Aldrich). The localization of GFP-NFAT was observed at an excitation wavelength of 488 nm with fluorescent microscopy (IX71, Olympus). More than 20 scenes were randomly scanned in each experiment and quantified the subcellular localization of GFP-NFAT using Photoshop (adobe systems).

2.10. Luciferase assays

NFAT-dependent luciferase activity and brain natriuretic peptide (BNP) promoter activity were measured as described previously (Fujii et al., 2005; Nishida et al., 2007, 2010). Cardiac myocytes were transiently co-transfected with 0.45 μg of pNFATLuc (Stratagene) and 0.05 μg of pRL-SV40 (Stratagene) control plasmid or with 0.3 μg of pBNP-Luc and 0.2 μg of pRL-SV40 using Fugene 6 (Roche Diagnostics) for 48 h followed by stimulation of AngII (100 nM) or ET-1 (100 nM). Luciferase activity was measured 6 h (for NFAT) or 24 h (for BNP) after the stimulation using dual luciferase reporter assay system (Promega) according to the manufacturer's protocol.

2.11. Measurement of mitochondrial [Ca^{2+}]

Mitochondrial [Ca^{2+}] was visualized using mitochondria-specific Ca^{2+} indicator, rhod-2/AM (Dojindo). Cardiac myocytes were loaded with 1 μM rhod-2/AM at 37 °C for 30 min. Then they were stimulated with AngII (100 nM) or ET-1 (100 nM), and the time course of fluorescence intensity was traced with a video image analysis system (Aquacosmos, Hamamatsu Photonics).

2.12. Measurement of hypertrophic response of cardiac myocytes

Hypertrophy of cells was assessed by a measurement of cell surface area and amount of actin filament, visualized by actin filament

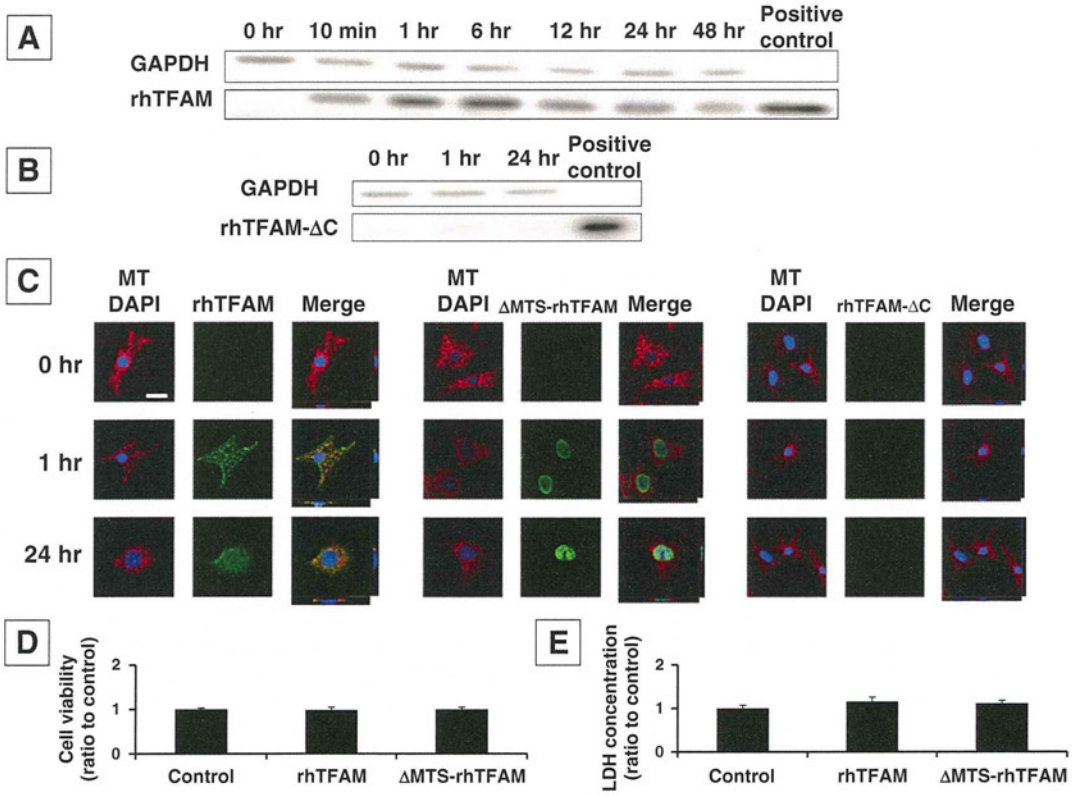

Fig. 2. The localization and cytotoxicity of rhTFAM proteins in cardiac myocytes. (A) Western blot analysis of myocytes treated with rhTFAM protein for 0–48 h. (B) Western blot analysis of myocytes treated with rhTFAM-ΔC protein for 0–24 h. (C) Confocal microscopic observations of myocytes treated with rhTFAM, ΔMTS-rhTFAM, or rhTFAM-ΔC. Red represents mitochondria (MT), green represents human TFAM (Alexa Fluor 488), and blue represents nucleus (DAPI). Scale bar = 20 μm. (D and E) The treatment with rhTFAM or ΔMTS-rhTFAM did not affect the cell viability (D) of myocytes and LDH concentration of the medium (E). Data are presented as ratio to control.

staining. Quantification of hypertrophy of myocytes was performed as previously described (Nishida et al., 2007, 2010). After AngII (100 nM) or ET-1 (100 nM) stimulation for 48 h, cells were fixed by 4% paraformaldehyde (nacalai tesque) and stained with Alexa Fluor 546 phalloidin (Invitrogen) for actin filaments visualization. Digital photographs were taken with confocal microscopy (FV-10i, Olympus) or Biozero Microscope (BZ-8000, Keyence), and the average values of the cell surface area and fluorescent intensity (more than 200 cells) were calculated using BZ-II Analyzer (Keyence).

2.13. Statistical analysis

Data are presented as mean ± standard error. Each experiment was repeated at least three times. Data were analyzed by a two-tailed Student's *t* test or analysis of variance followed by the Tukey post-hoc test with significance imparted at *P* values of <0.05.

3. Results

3.1. rhTFAM was recruited into the mitochondria of cardiac myocytes

We synthesized rhTFAM protein and investigated its recruitment into cardiac myocytes since we expected it as a new therapeutic modality. rhTFAM (100 nM) was just added to the culture medium of myocytes. rhTFAM protein rapidly entered into cultured rat neonatal ventricular myocytes within 10 min of the treatment, and remained in the cells even at 48 h (Fig. 2A). In contrast, rhTFAM-ΔC rarely entered into the cells (Fig. 2B). Confocal microscopy with z-scale analysis revealed that exogenously added rhTFAM localized both in the cytoplasm and mitochondria, whereas ΔMTS-rhTFAM was recruited mostly into the nucleus (Fig. 2C), both for 1 and 24 h treatment. These results suggested that MTS played an important role in determining the localization of recombinant TFAM in myocytes. We confirmed that rhTFAM-ΔC was not recruited into the cells (Fig. 2C), suggesting that some sequence in C-terminal tail of TFAM was important for the recruitment of this protein.

Moreover, ΔMTS-rhTFAM and rhTFAM had no significant cytotoxicity in cardiac myocytes at least at the concentration which we used in these experiments (100 nM), since cell viability did not alter (Fig. 2D) and LDH concentration in culture medium did not increase (Fig. 2E) after the treatment with ΔMTS-rhTFAM or rhTFAM.

3.2. rhTFAM increased mtDNA copy number and mtDNA-encoded proteins

In order to determine whether this recombinant protein functions in cardiac myocytes, we performed characterization of mitochondria after the treatment with rhTFAM. rhTFAM treatment increased mtDNA copy number dose-dependently (0–100 nM) with a maximum increase of approximately two-fold at 12 h, whereas mtDNA copy number was not affected by the treatment with ΔMTS-rhTFAM (Fig. 3A). We confirmed these results by two different PCR primer sets for mtDNA quantification and concluded that rhTFAM recruited into mitochondria functioned and directly increased mtDNA copy number. Using extract from empty vector, we ruled out the possibility that products other than rhTFAM from competent cells increased mtDNA contents (Fig. 3B). The treatment with rhTFAM or ΔMTS-rhTFAM (100 nM) for 24 h did not affect the morphology and the number of mitochondria significantly in cardiac myocytes (Fig. 3C).

To rule out the possibility that the recruitment and function of rhTFAM are the specific property of cardiac myocytes, we used another type of cell, RAW 264.7, to examine whether it also allows rhTFAM to enter into the cells. We found both rhTFAM and ΔMTS-rhTFAM were successfully recruited into RAW 264.7 cells (Fig. 4A and B). Subsequently, rhTFAM functioned to increase mtDNA copy number, but ΔMTS-rhTFAM did not (Fig. 4C). The recruitment and function of rhTFAM were similar to cardiac myocytes, suggesting that they were not unique properties of myocytes, but those of this specific protein.

In order to characterize the change of mitochondrial features by rhTFAM, we investigated the expression of mitochondrial electron transport complex proteins in cardiac myocytes. rhTFAM (100 nM)

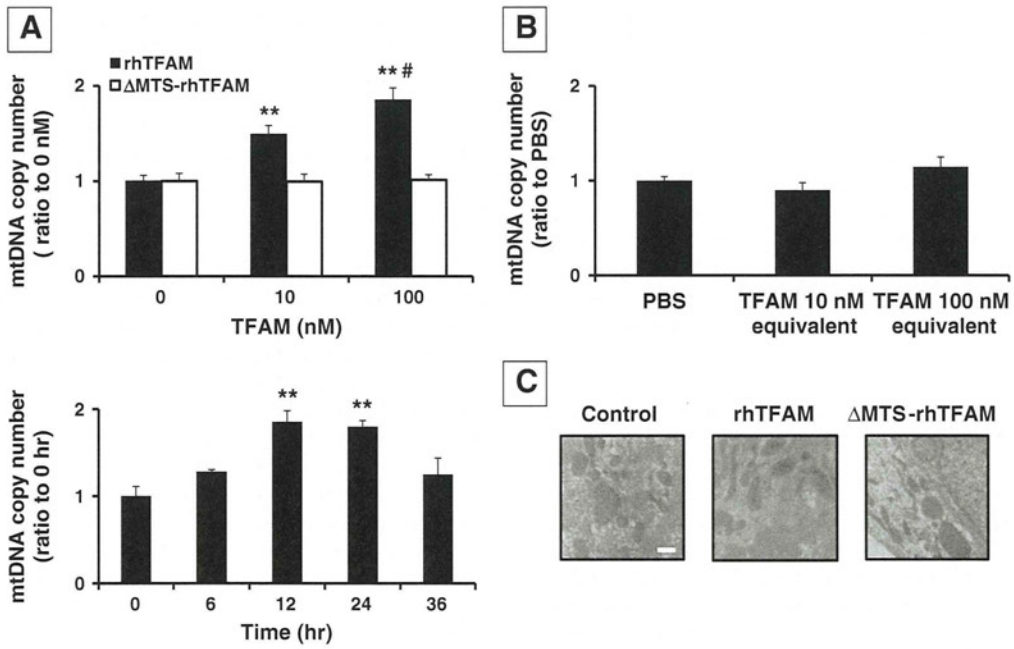

Fig. 3. The effects of rhTFAM on mitochondrial characteristics. (A) mtDNA copy number in myocytes treated with rhTFAM or ΔMTS-rhTFAM (0–100 nM) for 12 h, and rhTFAM (100 nM) for 0–36 h, quantified by real-time PCR relative to nucleus genome (ATIII gene). Data are presented as ratio to 0 nM or 0 h. **: $P<0.01$ vs. 0 nM or 0 h, #: $P<0.05$ vs. 10 nM. (B) mtDNA copy number of myocytes after the treatment with the product from empty vector. Myocytes were treated with the product from the empty vector by the equivalent volume of rhTFAM 10 or 100 nM, and mtDNA copy number was quantified. Data are shown as a ratio to buffer control (PBS). Values are mean ± SEM. (C) rhTFAM or ΔMTS-rhTFAM did not affect the morphology and number of mitochondria in cardiac myocytes, observed by TEM. Scale bar = 1 μm.

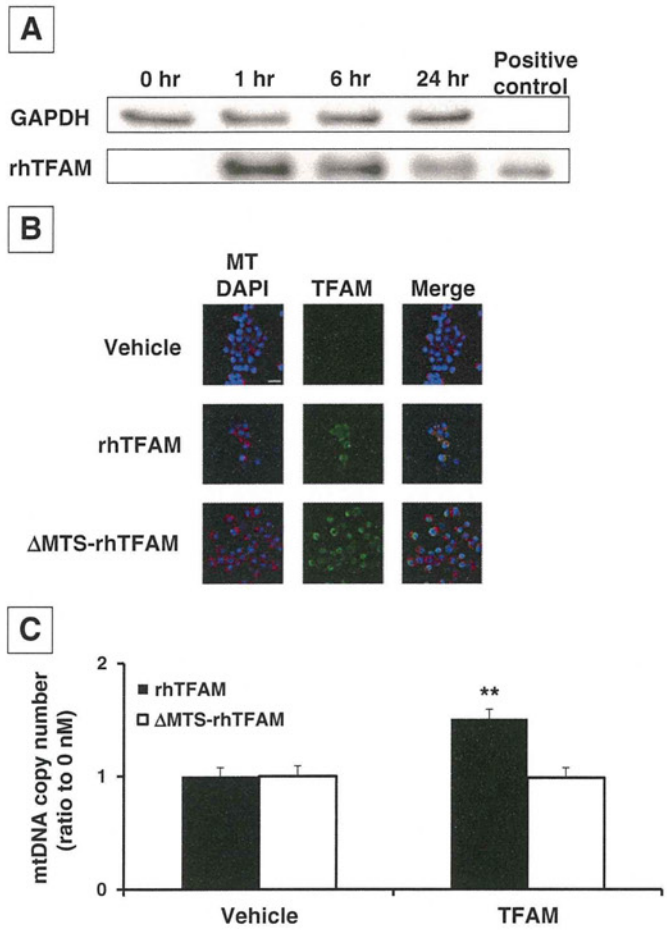

Fig. 4. The recruitment and function of rhTFAM on RAW 264.7 cells. (A) Western blot analysis of RAW 264.7 cells treated with rhTFAM protein for 0–24 h. (B) Confocal microscopic observations of RAW 264.7 cells treated with rhTFAM or ΔMTS-rhTFAM. Red represents mitochondria (MT), green represents human TFAM (Alexa Fluor 488), and blue represents nucleus (DAPI). Scale bar = 10 μm. (C) mtDNA copy number in RAW 264.7 cells treated with rhTFAM or ΔMTS-rhTFAM (50 nM) for 12 h, quantified by real-time PCR relative to nucleus genome (RPL27 gene). Data are presented as ratio to vehicle. **: $P<0.01$ vs. vehicle.

increased mtDNA-encoded COX I and COX III protein expression, which is a component of mitochondrial electron transport complex IV (Fig. 5A and B). In contrast, there were no increase of nuclear DNA-encoded NDUFA9 (complex I component) and SDHA (complex II component) protein contents (Fig. 5C and D). These results suggested that rhTFAM increased mtDNA copy number and subsequently increased mtDNA-encoded, but not nuclear DNA-encoded, mitochondrial proteins.

3.3. rhTFAM inhibited nuclear translocation of NFAT, NFAT transcriptional activity, and NFAT-dependent gene expression

Since overexpression of TFAM ameliorated post-MI remodeling in vivo, we expected rhTFAM also attenuated pathological hypertrophy and remodeling signals. The calcineurin/NFAT signaling pathway is a crucial signal that promotes pathological cardiac hypertrophy, both in vitro and in vivo (McKinsey and Kass, 2007; Molkentin, 2004; Vega et al., 2003). Dephosphorylation of NFAT by calcineurin, a Ca^{2+}-dependent serine/threonine phosphatase, induces cytosol-to-nucleus translocation, and NFAT functions as a transcriptional factor that activates many prohypertrophic genes. Furthermore, previous reports have suggested that the inhibition of NFAT signaling attenuated cardiac hypertrophy and failure (Sakata et al., 2000; van Rooij et al., 2004). We hypothesized that rhTFAM could also inhibit NFAT activation. We stimulated cardiac myocytes with AngII or ET-1, which are the major neurohumoral factors of pathological cardiac hypertrophy. First we investigated whether rhTFAM attenuated AngII- or ET-1-induced NFAT nuclear translocation using recombinant adenovirus encoding GFP-NFAT. The pretreatment with rhTFAM (100 nM) significantly inhibited AngII (100 nM)- or ET-1 (100 nM)-induced nuclear translocation of GFP-NFAT, whereas the pretreatment with ΔMTS-rhTFAM (100 nM) had no effect (Fig. 6A and B). This result suggested that recombinant TFAM recruited in mitochondria inhibited AngII- or ET-1-induced NFAT activation. Moreover, NFAT transcriptional activity as assessed by luciferase assay increased approximately 2.5-fold by stimulation with AngII (100 nM) or ET-1 (100 nM), and these increases were totally inhibited by the pretreatment with rhTFAM (10 nM) (Fig. 6C). The promoter activity of BNP gene, a NFAT-target gene widely used as marker of pathological cardiac hypertrophy, was also suppressed by rhTFAM (10 nM) (Fig. 6D). The expression of MCIP1 gene is also regulated by NFAT, and is used as a reporter gene of NFAT (Jin et al., 2010). MCIP1 mRNA expression was inhibited by the treatment with rhTFAM at baseline, just like TFAM-overexpression mice (Fig. 6E and F). These results confirmed that rhTFAM attenuated AngII- or ET-1-induced NFAT activation in cardiac myocytes.

We also investigated whether rhTFAM modulates MAPK p44/42 (ERK 1/2), another important pathway that induces cardiac hypertrophy (Aoki et al., 2000; McKinsey and Kass, 2007). The pretreatment with rhTFAM (100 nM) had no effect on ET-1 (100 nM)-induced MAPK p44/42 phosphorylation level (Fig. 7), suggesting that rhTFAM attenuates hypertrophy independent of MAPK signaling.

Since NFAT is regulated by the frequency of Ca^{2+} oscillation, we investigated the effect of rhTFAM on Ca^{2+} release from mitochondria. Stimulation with AngII (100 nM) or ET-1 (100 nM) decreased mitochondrial [Ca^{2+}] in cardiac myocytes, and rhTFAM (10 nM) significantly suppressed these decrease (Fig. 8). This result suggested that rhTFAM suppressed AngII- or ET-1-induced Ca^{2+} release from mitochondria to cytoplasm.

3.4. rhTFAM attenuated pathological hypertrophy of cardiac myocytes

Finally we examined whether rhTFAM subsequently attenuates hypertrophic response of myocytes. The treatment with rhTFAM (10 nM) significantly reduced the hypertrophic reactions induced by the stimulation with AngII (100 nM) or ET-1 (100 nM) for 48 h (Fig. 9A–C). We concluded that rhTFAM attenuates AngII- or ET-1-induced hypertrophy of cardiac myocytes.

4. Discussion

In our previous report we showed that, after MI, the overexpression of TFAM attenuated the decrease of mtDNA copy number, ameliorated pathological hypertrophy and improved survival rate dramatically (Ikeuchi et al., 2005). Thus from the clinical point of view, our next interest was to find the strategy to increase TFAM or mtDNA copy number efficiently. Accordingly, this report has mainly two novel findings. First, this is the first report showing that rhTFAM protein is successfully recruited into mitochondria of cardiac myocytes, and functions to increase mtDNA copy number. The other finding is that rhTFAM inhibits NFAT signaling and consequently attenuates morphological remodeling of cardiac myocytes. These results will enable novel new strategy to increase mtDNA copy number and attenuate pathological cardiac hypertrophy.

4.1. The recruitment of rhTFAM into cardiac myocytes

Previously it has been reported that recombinant TFAM with protein transduction domain was entered into cultured cells (Iyer et al., 2009). This study is the first report that rhTFAM which has the almost

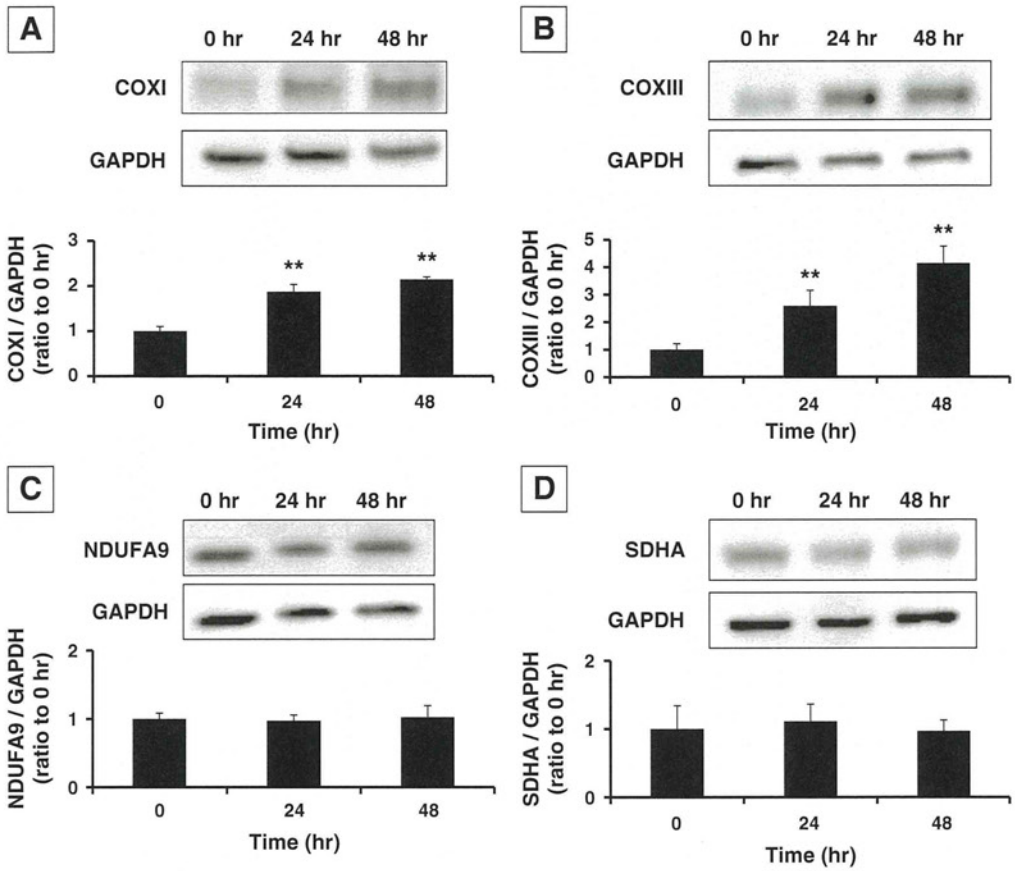

Fig. 5. The effects of rhTFAM on mitochondrial electron transport complex proteins. (A–D) The protein expression of COX I (A), COX III (B), NDUFA9 (C), and SDHA (D), 0–48 h after the treatment with rhTFAM. Data are presented as ratio to 0 h. **: $P<0.01$ vs. 0 h. Values are mean ± SEM.

identical amino acid sequence with native human TFAM can be successfully recruited into cardiac myocytes. Our result that rhTFAM-ΔC did not recruit into cells suggests that C-terminal tail of TFAM is responsible for this interesting property. Furthermore, we confirmed the recruitment and function of rhTFAM are independent of the cell types. The mechanism of its recruitment into cardiac myocytes remains unknown. Our data that rhTFAM entered into cells as early as 10 min, which was not inhibited in low temperature nor endocytosis inhibitors (data not shown), provides possibility that rhTFAM recruited into cytosol by a receptor-mediated pathway. Further investigations for the identification of the pathways for the recruitment of recombinant TFAM into the cells are necessary.

4.2. The effect of rhTFAM on mitochondrial characteristics

rhTFAM increased mtDNA copy number in myocytes (Fig. 3A) in a dose-dependent manner. Other than functioning as a transcription factor, endogenous TFAM regulates the amount of mtDNA by stabilizing mtDNA by forming a nucleoid structure (Kang et al., 2007). Considering the previous finding that the amount of mtDNA changes corresponding to the amount of TFAM, our results suggest that exogenously administered rhTFAM functioned similarly just like endogenous TFAM (Kanki et al., 2004). Furthermore, since ΔMTS-rhTFAM entered into myocytes but did not increase mtDNA copy number, it is likely that rhTFAM that entered mitochondria increased mtDNA copies. In this study, the mtDNA copy number peaked at 12 to 24 h after the rhTFAM treatment, and declined gradually thereafter. A single treatment with rhTFAM in myocytes prior to AngII or ET-1 stimulation successfully ameliorated pathological remodeling signals and subsequent pathological hypertrophy.

rhTFAM increased mtDNA-encoded, but not nuclear-encoded, mitochondrial proteins (Fig. 5). Probably it will be because of the increased mtDNA copy number, which is consistent with other's previous report that recombinant TFAM with protein transduction domain increased mitochondrial electron transport function and ATP synthesis in cultured cells (Thomas et al., 2011).

4.3. The effect of rhTFAM on NFAT signaling and pathological hypertrophy

The treatment with rhTFAM inhibited NFAT signaling in cardiac myocytes, and subsequent gene expression of MCIP1, which is a downstream of NFAT signaling, as well as in TFAM-overexpression mice hearts (Fig. 6E and F). The mechanism how rhTFAM inhibited AngII or ET-1-induced NFAT activation and hypertrophic response remains unknown. We need further investigation about the precise mechanism. Since mitochondria is known to participate in intracellular Ca^{2+} homeostasis via several Ca^{2+} uptake and release pathways (Bernardi, 1999), we speculated that rhTFAM inhibited Ca^{2+}/calcineurin-NFAT signaling by modulating $[Ca^{2+}]$. In fact, AngII or ET-1 induced the decrease of mitochondrial $[Ca^{2+}]$, suggesting the increase of Ca^{2+} release from mitochondria to cytoplasm, and rhTFAM inhibited AngII or ET-1-induced decrease of mitochondrial $[Ca^{2+}]$ (Fig. 8). However, the mechanism how rhTFAM inhibited AngII or ET-1-induced mitochondrial Ca^{2+} release still remains unknown. AngII is known to increase mitochondrial ROS in cardiac myocytes (Dai et al., 2011a, 2011b), and increased mitochondrial ROS is associated with mitochondrial Ca^{2+} release from mitochondria to cytoplasm (Kalivendi et al., 2005). rhTFAM inhibited superoxide production induced by rotenone, a complex I inhibitor, in cardiac myocytes (data not shown). Accordingly, the impact of rhTFAM on mitochondrial $[Ca^{2+}]$ might be associated with the inhibition of excessive mitochondrial ROS generation.

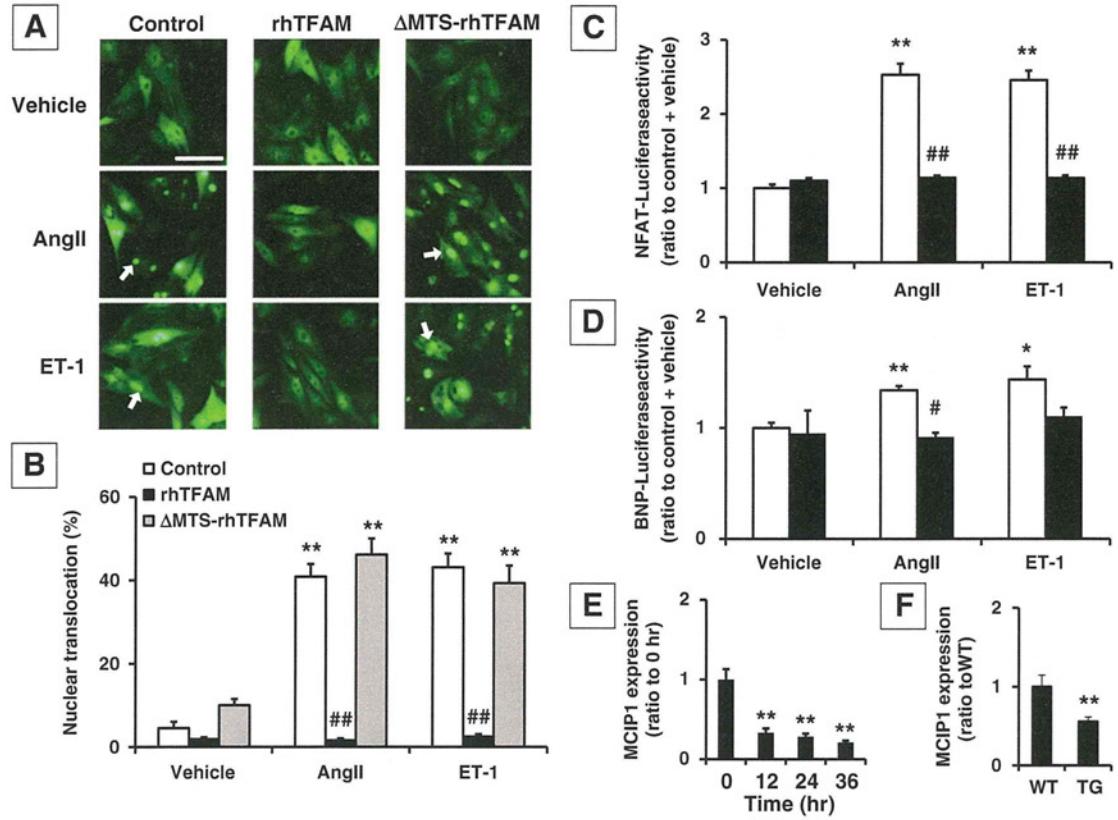

Fig. 6. The effects of rhTFAM on NFAT signaling. (A) The localization of GFP-NFAT protein in cardiac myocytes after the stimulation with AngII or ET-1. Arrows show GFP-NFAT translocated to nucleus. Scale bar = 50 μm. (B) rhTFAM significantly reduced the nuclear translocation rate of GFP-NFAT, whereas ΔMTS-rhTFAM had no effect on this translocation. (C and D) NFAT-luciferase activity (C) and BNP-luciferase activity (D) of myocytes stimulated with AngII or ET-1. NFAT- and BNP-luciferase activities were quantified as ratios to SV40 luciferase activity. Data are presented as ratio to control + vehicle. **: $P<0.01$, *: $P<0.05$ vs. control + vehicle; ##: $P<0.01$, #: $P<0.05$ vs. control. (E) MCIP1 mRNA expression in cardiac myocytes, 0–36 h after the treatment with rhTFAM. Data are presented as ratio to 0 h. **: $P<0.01$ vs. 0 h. (F) Cardiac MCIP1 mRNA expression of TFAM-overexpression mice and wild type littermates ($n=5$). WT means wild type mice, and TG means TFAM-overexpression mice. **: $P<0.01$ vs. WT. Values are mean ± SEM.

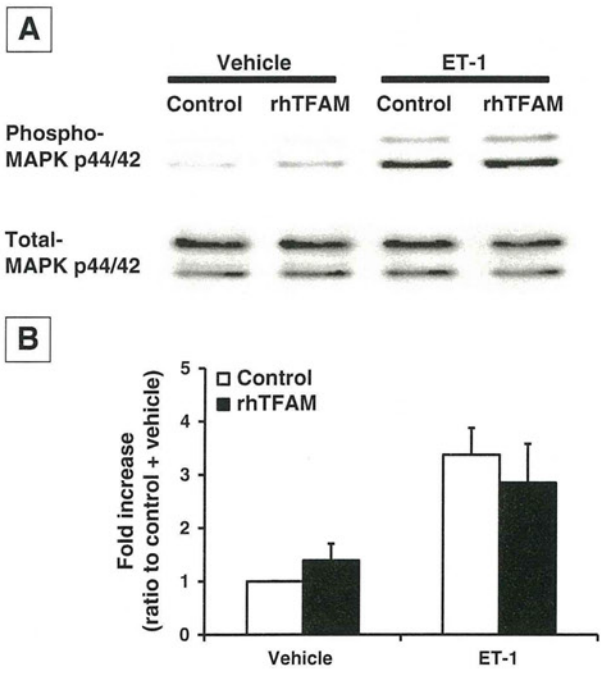

Fig. 7. The effects of rhTFAM on phosphorylation of MAPK p44/42. (A) Western blot analysis of myocytes probed with phospho-specific antibody and then reprobed for total protein. (B) The quantification of the ratio of phospho- to total-MAPK p44/42. The values were normalized to control + vehicle, and the data are shown as ratio to control + vehicle. Values are mean ± SEM.

NFAT signaling participates in pathological but not in physiological hypertrophy (Wilkins et al., 2004). Although hypertrophy has been traditionally viewed as a necessary first response to pathological stress but only later exacerbates disease, recent data suggest that hypertrophy in response to pathological stress may never be truly adaptive, and clinical studies support benefits from its inhibition (Frey et al., 2004; Gardin and Lauer, 2004; McKinsey and Kass, 2007). Moreover, the inhibition of NFAT signaling is reported to attenuate cardiac hypertrophy and failure (Sakata et al., 2000; van Rooij et al., 2004). Taken together, we believe that inhibiting NFAT signaling using rhTFAM can prevent cardiac hypertrophy and lead to the prevention of heart failure. We need further investigation, especially in vivo experiments, to confirm rhTFAM inhibits pathological cardiac hypertrophy and failure.

A possibility still exist that rhTFAM affected on other pathways besides NFAT signaling and subsequently inhibited AngII- or ET-1-induced hypertrophy of cardiac myocytes. However, we conclude in this study that exogenous rhTFAM have potential to increase mtDNA and inhibit pathological NFAT signaling in myocytes. Further elucidation of the precise mechanisms that TFAM functions in failing myocardium will be necessary.

5. Clinical implications

We propose in this report extreme novel findings that exogenously administered rhTFAM increased mtDNA copy number and attenuated pathological hypertrophy of cardiac myocytes. Thus rhTFAM could be a novel clinical strategy to increase mtDNA copy number and subsequently inhibit cardiac hypertrophy and failure. Further investigations of rhTFAM are anticipated.

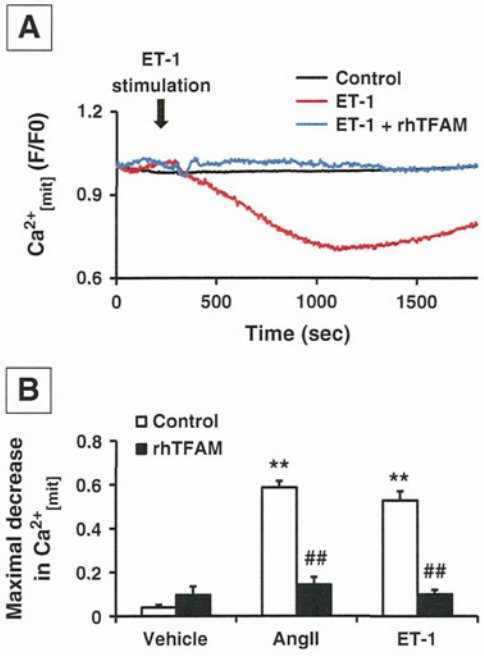

Fig. 8. The effects of rhTFAM on mitochondrial [Ca^{2+}]. (A) Representative trace of mitochondrial [Ca^{2+}] after the stimulation with ET-1, visualized using rhod-2. (B) rhTFAM significantly attenuated AngII- or ET-1-induced decrease of mitochondrial [Ca^{2+}]. **: $P<0.01$ vs. control + vehicle, ##: $P<0.01$ vs. control. Values are mean ± SEM.

Funding

This work was supported by Grant-in-Aid for Scientific Research (S) (23220013) and for Scientific Research (C) (23591084) from the Japan Society for the Promotion of Science.

Disclosures

None.

Acknowledgements

We thank Ms. Michiyo Tanaka for technical assistant. We appreciate the technical support from the Research Support Center, Graduate School of Medical Sciences, Kyushu University.

References

Alam, T.I., Kanki, T., Muta, T., Ukaji, K., Abe, Y., Nakayama, H., Takio, K., Hamasaki, N., Kang, D., 2003. Human mitochondrial DNA is packaged with TFAM. Nucleic Acids Res. 31, 1640–1645.

Aoki, H., Richmond, M., Izumo, S., Sadoshima, J., 2000. Specific role of the extracellular signal-regulated kinase pathway in angiotensin II-induced cardiac hypertrophy in vitro. Biochem. J. 347 (Pt 1), 275–284.

Bernardi, P., 1999. Mitochondrial transport of cations: channels, exchangers, and permeability transition. Physiol. Rev. 79, 1127–1155.

Dai, D.F., Chen, T., Szeto, H., Nieves-Cintron, M., Kutyavin, V., Santana, L.F., Rabinovitch, P.S., 2011a. Mitochondrial targeted antioxidant peptide ameliorates hypertensive cardiomyopathy. J. Am. Coll. Cardiol. 58, 73–82.

Dai, D.F., Johnson, S.C., Villarin, J.J., Chin, M.T., Nieves-Cintron, M., Chen, T., Marcinek, D.J., Dorn II, G.W., Kang, Y.J., Prolla, T.A., Santana, L.F., Rabinovitch, P.S., 2011b. Mitochondrial oxidative stress mediates angiotensin II-induced cardiac hypertrophy and Galphaq overexpression-induced heart failure. Circ. Res. 108, 837–846.

Frey, N., Katus, H.A., Olson, E.N., Hill, J.A., 2004. Hypertrophy of the heart: a new therapeutic target? Circulation 109, 1580–1589.

Fujii, T., Onohara, N., Maruyama, Y., Tanabe, S., Kobayashi, H., Fukutomi, M., Nagamatsu, Y., Nishihara, N., Inoue, R., Sumimoto, H., Shibasaki, F., Nagao, T., Nishida, M., Kurose, H., 2005. Galpha12/13-mediated production of reactive oxygen species is critical for angiotensin receptor-induced NFAT activation in cardiac fibroblasts. J. Biol. Chem. 280, 23041–23047.

Gardin, J.M., Lauer, M.S., 2004. Left ventricular hypertrophy: the next treatable, silent killer? JAMA 292, 2396–2398.

Garnier, A., Fortin, D., Delomenie, C., Momken, I., Veksler, V., Ventura-Clapier, R., 2003. Depressed mitochondrial transcription factors and oxidative capacity in rat failing cardiac and skeletal muscles. J. Physiol. 551, 491–501.

Hayashi, Y., Yoshida, M., Yamato, M., Ide, T., Wu, Z., Ochi-Shindou, M., Kanki, T., Kang, D., Sunagawa, K., Tsutsui, H., Nakanishi, H., 2008. Reverse of age-dependent

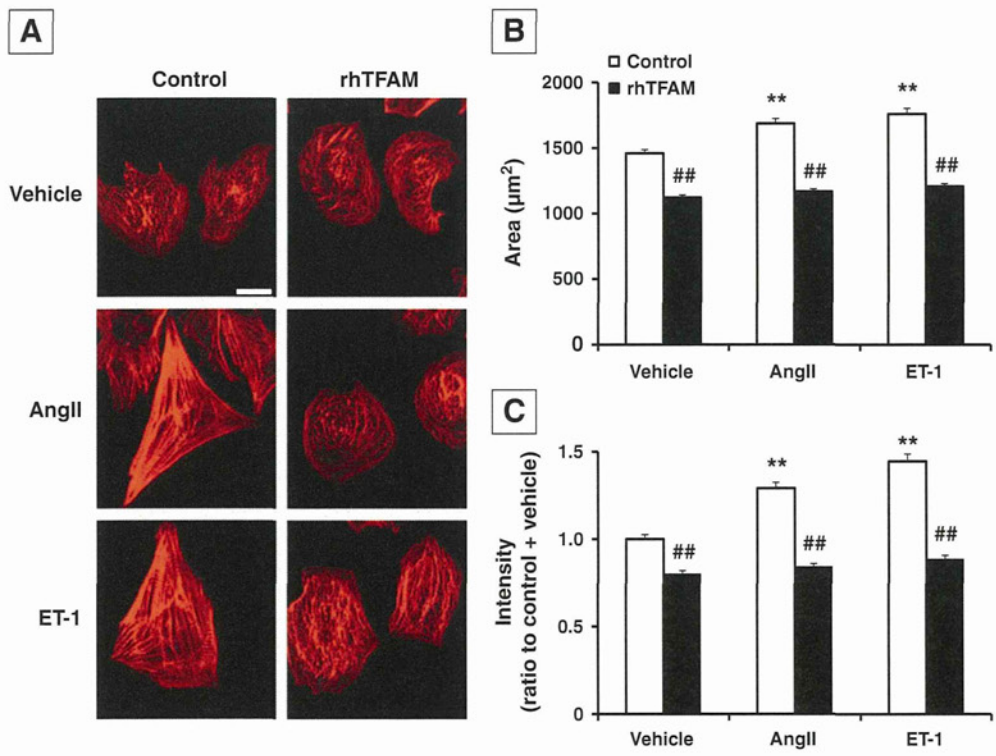

Fig. 9. Morphological remodeling of cardiac myocytes stimulated with AngII or ET-1. (A) Representative photomicrographs of AngII- or ET-1-stimulated myocytes immunostained using phalloidin. Scale bar = 20 μm. (B and C) Mean cell surface area (B) and fluorescent intensity (C) of 200–250 cells. **: $P<0.01$ vs. control + vehicle, ##: $P<0.01$ vs. control. Values are mean ± SEM.

memory impairment and mitochondrial DNA damage in microglia by an overexpression of human mitochondrial transcription factor a in mice. J. Neurosci. 28, 8624–8634.
Ide, T., Tsutsui, H., Hayashidani, S., Kang, D., Suematsu, N., Nakamura, K., Utsumi, H., Hamasaki, N., Takeshita, A., 2001. Mitochondrial DNA damage and dysfunction associated with oxidative stress in failing hearts after myocardial infarction. Circ. Res. 88, 529–535.
Ikeuchi, M., Matsusaka, H., Kang, D., Matsushima, S., Ide, T., Kubota, T., Fujiwara, T., Hamasaki, N., Takeshita, A., Sunagawa, K., Tsutsui, H., 2005. Overexpression of mitochondrial transcription factor a ameliorates mitochondrial deficiencies and cardiac failure after myocardial infarction. Circulation 112, 683–690.
Iyer, S., Thomas, R.R., Portell, F.R., Dunham, L.D., Quigley, C.K., Bennett Jr., J.P., 2009. Recombinant mitochondrial transcription factor A with N-terminal mitochondrial transduction domain increases respiration and mitochondrial gene expression. Mitochondrion 9, 196–203.
Jin, H., Hadri, L., Palomeque, J., Morel, C., Karakikes, I., Kaprielian, R., Hajjar, R., Lebeche, D., 2010. KChIP2 attenuates cardiac hypertrophy through regulation of Ito and intracellular calcium signaling. J. Mol. Cell. Cardiol. 48, 1169–1179.
Kalivendi, S.V., Konorev, E.A., Cunningham, S., Vanamala, S.K., Kaji, E.H., Joseph, J., Kalyanaraman, B., 2005. Doxorubicin activates nuclear factor of activated T-lymphocytes and Fas ligand transcription: role of mitochondrial reactive oxygen species and calcium. Biochem. J. 389, 527–539.
Kang, D., Kim, S.H., Hamasaki, N., 2007. Mitochondrial transcription factor A (TFAM): roles in maintenance of mtDNA and cellular functions. Mitochondrion 7, 39–44.
Kanki, T., Ohgaki, K., Gaspari, M., Gustafsson, C.M., Fukuoh, A., Sasaki, N., Hamasaki, N., Kang, D., 2004. Architectural role of mitochondrial transcription factor A in maintenance of human mitochondrial DNA. Mol. Cell. Biol. 24, 9823–9834.
Karamanlidis, G., Nascimben, L., Couper, G.S., Shekar, P.S., del Monte, F., Tian, R., 2010. Defective DNA replication impairs mitochondrial biogenesis in human failing hearts. Circ. Res. 106, 1541–1548.
Lagouge, M., Argmann, C., Gerhart-Hines, Z., Meziane, H., Lerin, C., Daussin, F., Messadeq, N., Milne, J., Lambert, P., Elliott, P., Geny, B., Laakso, M., Puigserver, P., Auwerx, J., 2006. Resveratrol improves mitochondrial function and protects against metabolic disease by activating SIRT1 and PGC-1alpha. Cell 127, 1109–1122.
Larsson, N.G., Wang, J., Wilhelmsson, H., Oldfors, A., Rustin, P., Lewandoski, M., Barsh, G.S., Clayton, D.A., 1998. Mitochondrial transcription factor A is necessary for mtDNA maintenance and embryogenesis in mice. Nat. Genet. 18, 231–236.
Li, H., Wang, J., Wilhelmsson, H., Hansson, A., Thoren, P., Duffy, J., Rustin, P., Larsson, N.G., 2000. Genetic modification of survival in tissue-specific knockout mice with mitochondrial cardiomyopathy. Proc. Natl. Acad. Sci. U. S. A. 97, 3467–3472.
McKinsey, T.A., Kass, D.A., 2007. Small-molecule therapies for cardiac hypertrophy: moving beneath the cell surface. Nat. Rev. Drug Discov. 6, 617–635.
Molkentin, J.D., 2004. Calcineurin-NFAT signaling regulates the cardiac hypertrophic response in coordination with the MAPKs. Cardiovasc. Res. 63, 467–475.
Nishida, M., Onohara, N., Sato, Y., Suda, R., Ogushi, M., Tanabe, S., Inoue, R., Mori, Y., Kurose, H., 2007. Galpha12/13-mediated up-regulation of TRPC6 negatively regulates endothelin-1-induced cardiac myofibroblast formation and collagen synthesis through nuclear factor of activated T cells activation. J. Biol. Chem. 282, 23117–23128.
Nishida, M., Watanabe, K., Sato, Y., Nakaya, M., Kitajima, N., Ide, T., Inoue, R., Kurose, H., 2010. Phosphorylation of TRPC6 channels at Thr69 is required for anti-hypertrophic effects of phosphodiesterase 5 inhibition. J. Biol. Chem. 285, 13244–13253.
Ohgaki, K., Kanki, T., Fukuoh, A., Kurisaki, H., Aoki, Y., Ikeuchi, M., Kim, S.H., Hamasaki, N., Kang, D., 2007. The C-terminal tail of mitochondrial transcription factor a markedly strengthens its general binding to DNA. J. Biochem. 141, 201–211.
Parisi, M.A., Clayton, D.A., 1991. Similarity of human mitochondrial transcription factor 1 to high mobility group proteins. Science 252, 965–969.
Sakata, Y., Masuyama, T., Yamamoto, K., Nishikawa, N., Yamamoto, H., Kondo, H., Ono, K., Otsu, K., Kuzuya, T., Miwa, T., Takeda, H., Miyamoto, E., Hori, M., 2000. Calcineurin inhibitor attenuates left ventricular hypertrophy, leading to prevention of heart failure in hypertensive rats. Circulation 102, 2269–2275.
Thomas, R.R., Khan, S.M., Portell, F.R., Smigrodzki, R.M., Bennett Jr., J.P., 2011. Recombinant human mitochondrial transcription factor A stimulates mitochondrial biogenesis and ATP synthesis, improves motor function after MPTP, reduces oxidative stress and increases survival after endotoxin. Mitochondrion 11, 108–118.
Tsutsumi, T., Ide, T., Yamato, M., Kudou, W., Andou, M., Hirooka, Y., Utsumi, H., Tsutsui, H., Sunagawa, K., 2008. Modulation of the myocardial redox state by vagal nerve stimulation after experimental myocardial infarction. Cardiovasc. Res. 77, 713–721.
van Rooij, E., Doevendans, P.A., Crijns, H.J., Heeneman, S., Lips, D.J., van Bilsen, M., Williams, R.S., Olson, E.N., Bassel-Duby, R., Rothermel, B.A., De Windt, L.J., 2004. MCIP1 overexpression suppresses left ventricular remodeling and sustains cardiac function after myocardial infarction. Circ. Res. 94, e18–e26.
Vega, R.B., Rothermel, B.A., Weinheimer, C.J., Kovacs, A., Naseem, R.H., Bassel-Duby, R., Williams, R.S., Olson, E.N., 2003. Dual roles of modulatory calcineurin-interacting protein 1 in cardiac hypertrophy. Proc. Natl. Acad. Sci. U. S. A. 100, 669–674.
Wang, J., Wilhelmsson, H., Graff, C., Li, H., Oldfors, A., Rustin, P., Bruning, J.C., Kahn, C.R., Clayton, D.A., Barsh, G.S., Thoren, P., Larsson, N.G., 1999. Dilated cardiomyopathy and atrioventricular conduction blocks induced by heart-specific inactivation of mitochondrial DNA gene expression. Nat. Genet. 21, 133–137.
Wilkins, B.J., Dai, Y.S., Bueno, O.F., Parsons, S.A., Xu, J., Plank, D.M., Jones, F., Kimball, T.R., Molkentin, J.D., 2004. Calcineurin/NFAT coupling participates in pathological, but not physiological, cardiac hypertrophy. Circ. Res. 94, 110–118.